Structure–Activity Relationships of Novel Iron Chelators for the Treatment of Iron Overload Disease: The Methyl Pyrazinylketone Isonicotinoyl Hydrazone Series

Danuta S. Kalinowski,[†] Philip C. Sharpe,[‡] Paul V. Bernhardt,*,[‡] and Des R. Richardson*,[†]

Iron Metabolism and Chelation Program, Department of Pathology, University of Sydney, Sydney, New South Wales 2006, Australia, and Centre for Metals in Biology, Department of Chemistry, University of Queensland, Brisbane, Queensland 4072, Australia

The design of novel Fe chelators with high Fe mobilization efficacy and low toxicity remains an important priority for the treatment of Fe overload disease. We have designed and synthesized the novel methyl pyrazinylketone isonicotinoyl hydrazone (HMPIH) analogs based on previously investigated aroylhydrazone chelators. The HMPIH series demonstrated high Fe mobilization efficacy from cells and showed limited to moderate antiproliferative activity. Importantly, this novel series demonstrated irreversible electrochemistry, which was attributed to the electron-withdrawing effects of the noncoordinating pyrazine N-atom. The latter functionality played a major role in forming redox-inactive complexes that prevent reactive oxygen species generation. In fact, the Fe complexes of the HMPIH series prevented the oxidation of ascorbate and hydroxylation of benzoate. We determined that the incorporation of electron-withdrawing groups is an important feature in the design of *N,N,O*-aroylhydrazones as candidate drugs for the treatment of Fe overload disease.

Introduction

The synthesis and design of novel iron (Fe) chelators is of great importance for the treatment of Fe-loading diseases such as β-thalassemia major.[1–5] This is due to the fact that treatment with the clinically used chelator, desferrioxamine (DFO[a]; Figure 1A), suffers many drawbacks that are partly caused by its high hydrophilicity.[5,6] This leads to poor absorption from the gastrointestinal tract, which necessitates subcutaneous administration for 12–24 h/day, 5–6 times/week to achieve a negative Fe balance.[7] In addition, a third of all patients treated with DFO experience swelling and pain at the injection site.[8,9] Cumulatively, these problems lead to poor patient compliance.

* To whom correspondence should be addressed. D.R. Richardson (Biology and Chemistry), Ph: +61-2-9036-6548. Fax: +61-2-9036-6549. E-mail: d.richardson@med.usyd.edu.au. P.V. Bernhardt (Chemistry), Ph: +61-7-3365-4266. Fax: +61-7-3365-4299. E-mail: p.bernhardt@uq.edu.au.
† University of Sydney.
‡ University of Queensland.
[a] Abbreviations: 3-AP, 3-aminopyridine-2-carboxaldehyde thiosemicarbazone; DFO, desferrioxamine; HDp44mT, di-2-pyridylketone 4,4-dimethyl-3-thiosemicarbazone; HMPAH, methyl pyrazinylketone *p*-aminobenzoyl hydrazone; HMPBH, methyl pyrazinylketone benzoyl hydrazone; HMP3BBH, methyl pyrazinylketone *m*-bromobenzoyl hydrazone; HMP4BBH, methyl pyrazinylketone *p*-bromobenzoyl hydrazone; HMPHH, methyl pyrazinylketone *p*-hydroxybenzoyl hydrazone; HMPIH, methyl pyrazinylketone isonicotinoyl hydrazone; HMPNH, methyl pyrazinylketone *p*-nitrobenzoyl hydrazone; HMPTH, methyl pyrazinylketone thiophenecarboxyl hydrazone; HMPTFH, methyl pyrazinylketone *p*-trifluoromethylbenzoyl hydrazone; H₂NIH, 2-hydroxy-1-naphthaldehyde isonicotinoyl hydrazone; HPCAH, 2-pyridylcarboxaldehyde *p*-aminobenzoyl hydrazone; HPCBH, 2-pyridylcarboxaldehyde benzoyl hydrazone; HPC3BBH, 2-pyridylcarboxaldehyde *m*-bromobenzoyl hydrazone; HPC4BBH, 2-pyridylcarboxaldehyde *p*-bromobenzoyl hydrazone; HPCHH, 2-pyridylcarboxaldehyde *p*-hydroxybenzoyl hydrazone; HPCIH, 2-pyridylcarboxaldehyde isonicotinoyl hydrazone; HPCNH, 2-pyridylcarboxaldehyde *p*-nitrobenzoyl hydrazone; HPCTH, 2-pyridylcarboxaldehyde thiophenecarboxyl hydrazone; HPCTFH, 2-pyridylcarboxaldehyde *p*-trifluoromethylbenzoyl hydrazone; H₂PIH, pyridoxal isonicotinoyl hydrazone; HPKAH, di-2-pyridylketone *p*-aminobenzoyl hydrazone; HPKBH, di-2-pyridylketone benzoyl hydrazone; HPK3BBH, di-2-pyridylketone *m*-bromobenzoyl hydrazone; HPK4BBH, di-2-pyridylketone *p*-bromobenzoyl hydrazone; HPKIH, di-2-pyridylketone isonicotinoyl hydrazone; HPKHH, di-2-pyridylketone *p*-hydroxybenzoyl hydrazone; HPKNH, di-2-pyridylketone *p*-nitrobenzoyl hydrazone; HPKTH, di-2-pyridylketone thiophenecarboxyl hydrazone; HPKTFH, di-2-pyridylketone *p*-trifluoromethylbenzoyl hydrazone; IBE, iron-binding equivalent; ROS, reactive oxygen species; Tf, transferrin.

Deferiprone (Figure 1A) is an orally active Fe chelator that is available in a number of countries for the treatment of Fe overload disease.[10] However, its safety remains controversial due to a number of conflicting studies reporting liver fibrosis.[11–14] More recently, the triazole, 4-[3,5-bis(2-hydroxyphenyl)-1,2,4-triazol-1-yl]benzoic acid, has gained FDA approval as an orally active Fe chelator.[15] However, the Fe chelation efficacy and safety of the drug remains unclear.[16] Therefore, the development of new, efficient, and safe orally active Fe chelators is necessary for the treatment of Fe overload disease.

One previously synthesized group of Fe chelators developed within our laboratory, the 2-pyridylcarboxaldehyde isonicotinoyl hydrazone (HPCIH; Figure 1B) analogs, were derived from the parent compound of the same name. These ligands demonstrated high Fe mobilization efficacy and were able to effectively prevent Fe uptake from the Fe transport protein, transferrin (Tf), in vitro.[17,18] Of this series, 2-pyridylcarboxaldehyde benzoyl hydrazone (HPCBH; Figure 1B), 2-pyridylcarboxaldehyde *m*-bromobenzoyl hydrazone (PC3BBH; Figure 1B), and 2-pyridylcarboxaldehyde thiophenecarboxyl hydrazone (HPCTH; Figure 1B) were most effective at mobilizing intracellular Fe and preventing Fe uptake in the SK-N-MC neuroepithelioma cell line.[17] Another in vitro study using a model of mitochondrial Fe overload illustrated that HPCIH was the most effective of this series at increasing Fe release from the mitochondria, which is an important factor in the potential treatment of the disease, Friedreich's ataxia.[19]
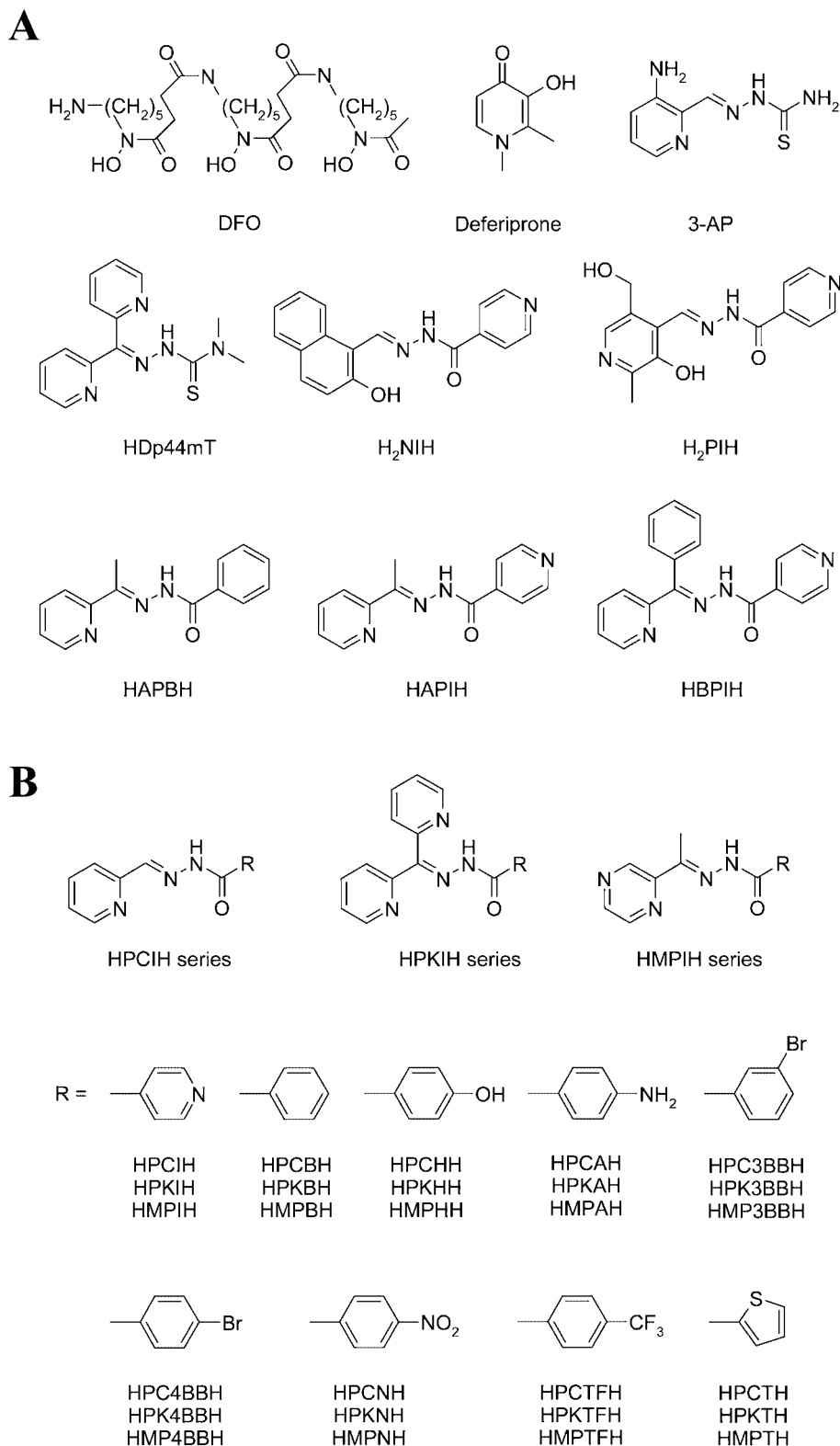
More recently, an in vivo mouse trial was completed illustrating the ability of HPCTH to induce substantial levels of Fe excretion when administered orally.[20] In fact, the efficacy of HPCTH was comparable to that of deferiprone at the same dose.[20] The HPCIH ligands were found to have little antiproliferative activity (IC$_{50}$ 40–50 μM) in vitro against the SK-N-MC neuroepithelioma cell line, with an effect similar to that of DFO.[17] For a ligand to be ideal for the treatment of Fe overload disease it must not exhibit marked antiproliferative effects nor increase redox activity upon complexation with Fe. As such, the HPCIH series meets the necessary criteria needed for the treatment of Fe overload disease.

Figure 1. Chemical structures of iron chelators described in this study. (A) Desferrioxamine (DFO), deferiprone, 3-aminopyridine-2-carboxaldehyde thiosemicarbazone (3-AP), di-2-pyridylketone 4,4-dimethyl-3-thiosemicarbazone (HDp44mT), 2-hydroxy-1-naphthylaldehyde isonicotinoyl hydrazone (H$_2$NIH), pyridoxal isonicotinoyl hydrazone (H$_2$PIH), 2-acetylpyridine benzoyl hydrazone (HAPBH), 2-acetylpyridine isonicotinoyl hydrazone (HAPIH), and 2-benzoylpyridine isonicotinoyl hydrazone (HBPIH). (B) The chemical structures of members of the 2-pyridylcarboxaldehyde isonicotinoyl hydrazone (HPCIH), di-2-pyridylketone isonicotinoyl hydrazone (HPKIH), and methyl pyrazinylketone isonicotinoyl hydrazone (HMPIH) series.

Considering the high Fe chelation efficacy of the HPCIH analogs, a novel series of ligands were developed to incorporate the more lipophilic di-2-pyridylketone moiety because lipophilicity and membrane permeability play a critical role in Fe chelation efficacy.[5,21] These tridentate chelators, namely, the

di-2-pyridylketone isonicotinoyl hydrazone (HPKIH; Figure 1B) series, were found to effectively promote the efflux of intracellular Fe and inhibit the uptake of Fe from Tf by tumor cells in culture.[22] More importantly, this series of ligands showed much higher antiproliferative activity (IC$_{50}$ 1–42 μM) than their

parent HPCIH analogs.[22] Interestingly, the HPKIH series were found to act via a different mechanism to that of their HPCIH counterparts.[23] The $Fe^{II}(PKIH)_2$ complexes in the presence of H_2O_2 were able to stimulate benzoate hydroxylation and plasmid DNA degradation.[23,24] Cyclic voltammetry of the Fe^{II} complexes from the HPKIH series revealed that they are capable of undergoing redox cycling with quasi-reversible $Fe^{III/II}$ redox couples being identified in the presence of water.[23] This is in contrast to what has been observed with the $Fe(PCIH)_2$ analogs, which show totally irreversible electrochemistry due to susceptibility of the Fe^{III} complexes to attack by water, leading to a complex that is resistant to reduction.[18] Overall, these studies suggested that redox cycling of $Fe(PKIH)_2$ and its analogous complexes played a role in their antiproliferative activity through the generation of damaging reactive oxygen species (ROS).

In an attempt to develop novel chelators with high Fe mobilization efficacy for the treatment of Fe overload disease, in this study we synthesized the methyl pyrazinylketone isonicotinoyl hydrazone (HMPIH; Figure 1B) series. These ligands were designed to contain the methyl pyrazinylketone moiety to investigate its effect on Fe mobilization and antiproliferative activity. The effect of this structural modification on the activity of these chelators is assessed in comparison to chelators of the HPCIH and HPKIH classes.

Results and Discussion

Synthesis and Characterization of the HMPIH Series. The chelators of the HMPIH series were readily prepared via a Schiff base condensation reaction of methyl pyrazinylketone with the appropriate hydrazide, as reported for other related aroylhydrazone analogs.[23]

Several members of this novel series were further characterized crystallographically. The molecular structures of HMPBH, HMPHH, and HMPTFH are shown in Figure 2A−C in various orientations, and their crystal data are presented in Table 1. All molecules exhibit similar conformations. The methyl groups are *syn* with respect to N1. The driving force for this conformation is to avoid H···H repulsion between the methyl group and the H-atom attached to C2. In the conformations seen, the C2−H2 group is *syn* with N3, which bears no proton thus accommodating the proximate aryl proton. All ligands are close to planar. The greatest deviations from ideally planar dihedral angles are seen about the O1−C7−C8−C13 group, which span the range 14–25°. By contrast, the acetylpyrazine moiety is closer to planarity (N1−C1−C5−C6 < 14°).

H-bonding is different in all three structures. Interestingly, there are no classical H-bonds in HMPBH. The only potential H-bond donor (N4-H4A) is sterically hindered by the adjacent methyl group and cannot interact with any of the potential H-bond acceptors (N1, N2, N3, or O1). The unhindered 4-hydroxyl group on HMPHH leads to a polymer connected by intermolecular H-bonds (O2-H2A···O1). The structure of HMPTFH is similar to HMPBH with only a very weak intermolecular H-bond (N4-H4···O1′ 2.64 Å symmetry operator: *x* + 1, *y*, *z*). The trifluoromethyl group was rotationally disordered (not shown in Figure 2C), but this was isolated to this residue.

Although the ligands from this series are potentially tridentate (*N,N,O*) chelators, the conformation of each molecule in Figure 2A−C finds one of the donor atoms (N1) *anti* to the other donor atoms (N3 and O1), and the C=N bond defines the *E*-isomeric form where N4 is *trans* to the pyrazine ring. A similar conformation is found with other aroylhydrazones of this type, such as the HPCIH class.[25,26] As a consequence, the molecule
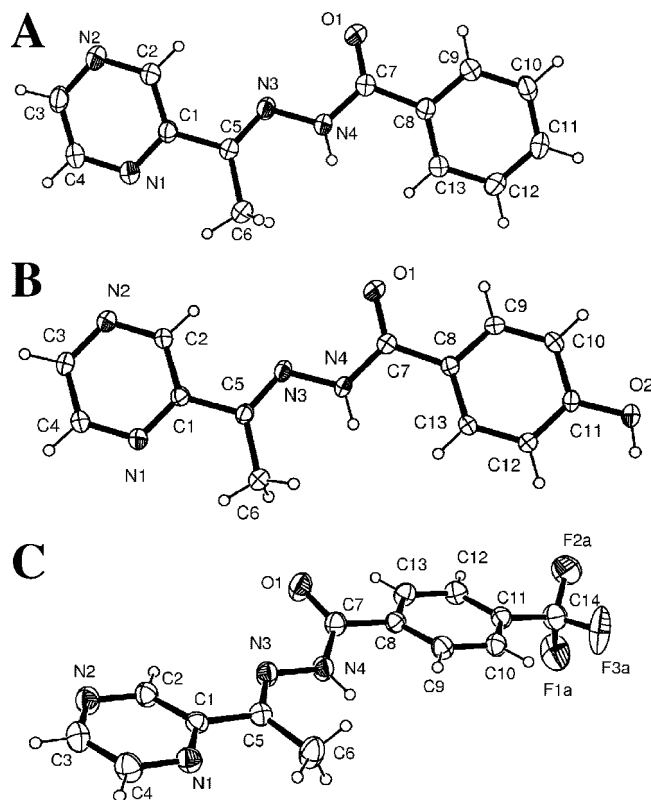
Figure 2. ORTEP diagrams of (A) HMPBH, (B) HMPHH, and (C) HMPTFH (30% probability ellipsoids shown).

Table 1. Crystal Data

	HMPBH	HMPHH	HMPTFH
formula	$C_{13}H_{12}N_4O$	$C_{13}H_{12}N_4O_2$	$C_{14}H_{11}F_3N_4O$
mol. wt	240.27	256.27	308.27
crystal system	triclinic	triclinic	monoclinic
a (Å)	7.471(1)	7.9667(8)	5.4266(9)
b (Å)	8.1965(8)	8.234(1)	31.837(7)
c (Å)	9.852(1)	9.513(1)	7.757(3)
α (°)	77.088(9)	94.59(2)	
β (°)	82.30(2)	101.97(1)	95.90(3)
γ (°)	79.64(1)	105.31(1)	
V (Å³)	575.7(1)	582.8(1)	1333.1(6)
T (K)	293(2)	293(2)	293(2)
Z	2	2	4
space group	$P\bar{1}$	$P\bar{1}$	$P\,2_1/n$
μ (mm^{-1})	0.093	0.103	0.130
indep. refs (R_{int})	1992 (0.0180)	2027 (0.0160)	2341 (0.0435)
R_1 (obs. data)	0.0396	0.0434	0.0519
wR_2 (all data)	0.1279	0.1382	0.1710
CCDC No.	656689	656690	656691

is favorably disposed to coordinate a metal ion through the pyridyl N-atom (N1), imine N-atom (N3), and carbonyl O-atom (O1) after rotation of the pyrazine group by 180° about C1–C5. It is suggested that this rotation could occur in solution, thus allowing the HMPIH ligands to bind Fe, as evident from the synthesis of the HMPIH Fe complexes in good yield (see below).

The ¹H NMR spectra of the HMPIH series indicated that the *E*-conformation was preserved in solution due to the shielded amide proton resonance. The corresponding *Z*-isomer enables an intramolecular H-bond between the NH group and the N-atom on the heterocyclic ring and the NH group appears well downfield as a consequence.[23] The existence of the *E*-isomer in solution confers the appropriate stereochemistry to enable Fe chelation. This is relevant as the existence in solution of

Table 2. Octanol–Water Partition Coefficients (Log P) for the HMPIH Series

ligand	log P
HMPBH	1.9
HMPIH	1.2
HMP3BBH	2.9
HMP4BBH	2.9
HMPHH	1.9
HMPAH	1.3
HMPTFH	2.0
HMPNH	2.1
HMPTH	2.6

Table 3. $Fe^{III/II}$ Redox Potentials in DMF and in 70:30 DMF/H_2O (v/v; Anodic Potentials Shown)

Fe^{II} complex	100% DMF $E^{o\prime}$ (mV vs $Fc^{+/0}$)	70:30 DMF/H_2O (v/v) E_{pa} (mV vs NHE)
$Fe^{II}(MPIH)_2$	+16	+642
$Fe^{II}(MPBH)_2$	−63	+578
$Fe^{II}(MP3BBH)_2$	−20	+610
$Fe^{II}(MP4BBH)_2$	−32	+592
$Fe^{II}(MPTFH)_2$	−5	+569
$Fe^{II}(MPNH)_2$	+23	+588
$Fe^{II}(MPTH)_2$	−92	+599

the Z-isomer of a related chelator, namely, 2-benzoylpyridine isonicotinoyl hydrazone (HBPIH; Figure 1A) leads to poor Fe chelation efficacy.[27] Interestingly, the amide proton peak of the HMPIH chelators was found to be sensitive to the identity of the hydrazide moiety. The most deshielded NH peak was observed with HMPNH (11.41 ppm), which contained the strongly electron-withdrawing nitro substituent. Conversely, the most shielded NH resonance was exhibited by HMPAH (10.50 ppm), containing the electron-donating amino substituent. The pyrazine proton resonances were largely unaffected by the inductive effects of the hydrazide moiety, with little variation observed between members of the HMPIH series.

Partition Coefficients of the Free Ligands. The octanol–water partition coefficients for the HMPIH series were determined using methods reported previously by our laboratories.[28] This was important to determine as chelator lipophilicity is known to be a relevant factor in terms of their Fe mobilization efficacy and antiproliferative activity.[21] The log P values of the HMPIH series (Table 2) varied from 1.2 (HMPIH) to 2.9 (HMP3BBH and HMP4BBH), with many ligands having values that are in the optimal range necessary for maximum Fe mobilization.[29] The log P values correlated with the identity of their aromatic substituents, with ligands containing the hydrophobic Br substituent showing large log P values, while the hydrophilic HMPAH ligand demonstrated a lower log P value.

Synthesis and Characterization of the HMPIH Fe Complexes. To confirm the Fe binding ability of the HMPIH series, their Fe^{II} complexes were synthesized and characterized. This was readily achieved by the addition of the ferrous salt to a basic solution of the ligand in a 1:2 ratio to give a charge-neutral, *bis*-ligand Fe^{II} complex in good yield. The analytically pure Fe complexes were characterized by NMR, IR, and UV–vis spectroscopy.

In each case, the chelators bind Fe as a tridentate ligand, and the NH group adjacent to the carbonyl deprotonates to generate an enolate form of the ligand. This was confirmed through the IR spectra of their Fe^{II} complexes, which demonstrated the loss of the carbonyl vibration at 1648–1683 cm^{-1}, evident in the spectra of their free ligands. Strong bands in the IR spectra of the Fe^{II} complexes appearing between 1261 and 1600 cm^{-1} can be partly attributed to the formation of the Fe−O−C=N group. The electronic and IR spectra of these complexes are typical of other pyridine hydrazone relatives.[23] The electronic spectra of the HMPIH series Fe^{II} complexes are similar and are dominated by charge transfer transitions. The complexes exhibit a dark green color due to a metal to ligand charge transfer transition that occurs at 650–700 nm. This characteristically asymmetric electronic absorption peak is a common feature of the Fe^{II} complexes from the HPCIH, HPKIH, HAPIH series and these complexes as well. The Fe^{II} complexes were all diamagnetic, and relatively sharp ^{1}H NMR spectra were obtained in contrast to the spectra of the Fe complexes of the HPCIH analogs, which

are very significantly paramagnetically broadened and downfield shifted. As the substituent group increased in electron-withdrawing ability, there was a slight increase in paramagnetic broadening, with the $Fe(MPNH)_2$, $Fe(MPTFH)_2$, and $Fe(MP4BBH)_2$ complexes being the most affected.

Electrochemistry of the Fe Complexes. An essential property of a potential Fe chelator for the treatment of Fe overload disease is its ability to bind Fe without promoting the generation of damaging ROS through Fenton chemistry, which would most likely lead to cytotoxicity.[30] An indicator of the potential for these complexes to undergo redox cycling in a physiological context is provided by examination of their redox potentials.

First, the $Fe^{III/II}$ redox potentials were determined in DMF to gauge the relative inductive effects of the noncoordinating aromatic and heterocyclic substituents on the metal center. In DMF, all complexes exhibited reversible $Fe^{III/II}$ couples (Table 3). The redox potential of $Fe(MPAH)_2$ was not measured due to its extremely low solubility. The potentials using a glassy carbon electrode spanned a range of 115 mV, from $[Fe(MPTH)_2]^{+/0}$ at −92 mV to $[Fe(MPNH)_2]$ at 23 mV versus ferrocene/ferrocenium ($Fc^{+/0}$). As expected, there was a general trend to higher potentials in the presence of more electron-withdrawing substituents. As well as a metal-centered process, the complexes also displayed a ligand-centered reduction process around −1500 mV, with the exception of $Fe(MPNH)_2$, where nitro group reduction occurred around −1400 mV and the one electron pyrazine reduction was shifted cathodically to −1700 mV.

In contrast to the nonaqueous electrochemistry above, all Fe complexes of the HMPIH series examined demonstrated irreversible $Fe^{III/II}$ couples in aqueous/DMF solution (E_{pa} +569 to +642 mV vs NHE; Table 3; Figure 3). This irreversible electrochemistry indicates that the Fe^{II} complexes of the HMPIH series are unable to catalyze the generation of ROS, which requires the continual regeneration of Fe^{II} following oxidation by peroxide. The electrochemistry of the HMPIH series was similar to that of the related HPCIH analogs. In fact, the Fe^{II} complexes of the HPCIH chelators also demonstrated irreversible $Fe^{III/II}$ electrochemistry at comparable potentials.[18]

Significantly, the electrochemistry of the structurally related 2-acetylpyridine benzoyl hydrazone (HAPBH; Figure 1A) and 2-acetylpyridine isonicotinoyl hydrazone (HAPIH; Figure 1A) Fe complexes demonstrate completely different electrochemical properties.[27] Structurally, these ligands are very similar to that of the HMPIH series, except the former set of chelators contain a coordinating pyridine ring, while the HMPIH analogs contain an additional N atom of the chelating pyrazine ring (Figure 1B). Unlike the HMPIH series, these 2-acetylpyridine isonicotinoyl hydrazone ligands demonstrated quasi-reversible $Fe^{III/II}$ responses, suggesting that redox activity may play an important role in their antiproliferative activity.[27] Indeed, their $Fe^{III/II}$ redox potentials were lower than that of their related HPKIH analogs.[23]
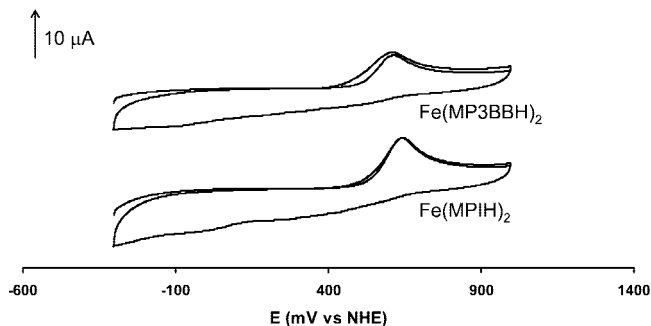
Figure 3. Cyclic voltammograms of the Fe complexes of selected members of the HMPIH series, namely, Fe(MP3BBH)$_2$ and Fe(MPIH)$_2$; sweep rate 200 mVs^{-1}, solvent 70:30 DMF/H$_2$O (v/v) with 0.1 M NaClO$_4$.

This was consistent with the electron-donating inductive effects of the methyl group attached to the imine C-atom in comparison with the electron-withdrawing 2-pyridyl ring of the HPKIH series.[27] It was suggested that the methyl group played a role in their reversible electrochemistry in comparison to that of the H-atom of the HPCIH analogs, preventing attack by the hydroxyl anion and leading to a reversible redox couple.[27] Comparatively, these results clearly suggest that the electron-withdrawing effects of the additional pyrazine N-atom of the HMPIH series acts in a similar manner to that of the pyridyl ring of the HPKIH series, resulting in higher potentials and irreversible Fe$^{III/II}$ redox electrochemistry. Therefore, it is important to consider the incorporation of electron-withdrawing substituents in the design of *N,N,O* aroylhydrazone ligands for the treatment of Fe overload disease. Such irreversible electrochemistry is an important factor that needs to be considered for the creation of nonredox active chelators for the treatment of Fe overload disease.

This property of the HMPIH series Fe complexes is in marked contrast to the reversible electrochemistry, which is observed for chelators of the DpT and BpT class[31,32] that have potential as antitumor agents.[33,34] The redox potentials ($E°$ +99 − +225 mV vs NHE) of this latter group of ligands[31,32] enable the facile generation of ROS under biological conditions, which may play a key role in their marked antiproliferative activity against tumor cells.[31,33,34] Hence, by manipulating the redox activity of these compounds, ligands can be designed as novel anticancer therapeutics where this property aids antitumor activity. Alternatively, for the treatment of Fe overload, the Fe complexes should be redox-inactive, which correlates to low antiproliferative efficacy.[30]

In summary, the electron-withdrawing effects of the additional pyrazine N-atom resulted in irreversible electrochemistry and demonstrates the potential suitability of the HMPIH series as effective protective agents for the treatment of Fe overload disease.

Biological Studies. Cellular Fe Efflux. For an Fe chelator to have potential as an agent for the treatment of Fe overload, it must be able to effectively mobilize intracellular Fe without inducing antiproliferative activity.[30] Thus, the ability of the HMPIH series to induce intracellular ^{59}Fe efflux from prelabeled SK-N-MC neuroepithelioma cells was assessed. This cell line was chosen as its Fe metabolism is well characterized and it has been used to examine the effect of other chelators on Fe mobilization and Fe uptake.[21,33,35,36] The ability of the HMPIH series to release intracellular ^{59}Fe was compared to that of a number of control compounds, including (1) their corresponding HPCIH and HPKIH analogs (Figure 1B),[17,22,23] (2) the chelator,

pyridoxal isonicotinoyl hydrazone (H$_2$PIH; Figure 1A), known for its high Fe mobilization efficacy,[17,21,22,37,38] (3) the ligand, 2-hydroxy-1-naphthaldehyde isonicotinoyl hydrazone (H$_2$NIH; Figure 1A), which also exhibits high Fe mobilization activity,[21,35,39] and (4) DFO (Figure 1A), the current standard treatment for Fe overload disease.[5,40]

As previously demonstrated,[31,32] the positive controls, H$_2$PIH and H$_2$NIH, markedly increased ^{59}Fe release, mobilizing 40 ± 1% and 44 ± 1% of cellular ^{59}Fe, respectively (Figure 4A). On the other hand, the highly hydrophilic chelator, DFO, exhibited limited ability to promote ^{59}Fe mobilization, as previously described,[32,36] releasing 16 ± 1% of intracellular ^{59}Fe (Figure 4A). In comparison, control medium alone resulted in only 6 ± 1% of ^{59}Fe release (Figure 4A).

In Figure 4A,B, the Fe chelation efficacy of each member of the HMPIH group is directly compared to the activity of the relevant analog of the HPCIH and HPKIH series. All members of the HMPIH series demonstrated high levels of ^{59}Fe mobilization efficacy, mediating the release of 31–45% of cellular ^{59}Fe (Figure 4A). In fact, HMPIH and HMPTH, showed comparable ($p > 0.05$) ^{59}Fe mobilizing activity to that of H$_2$NIH. The ligands, HMPTH, HMPIH, HMP4BBH, and HMPHH, demonstrated significantly ($p < 0.05$) higher or comparable levels of ^{59}Fe release to that of the positive control, H$_2$PIH (Figure 4A). DFO was significantly ($p < 0.001$) less effective than all members of the HMPIH series. Interestingly, no correlation was observed between the log P value of the HMPIH ligands and their ability to mobilize cellular ^{59}Fe, suggesting that other factors are important in this process.

The majority of the HMPIH series exhibited significantly ($p < 0.005$) enhanced or comparable levels of cellular ^{59}Fe release to that of their corresponding HPCIH analogs,[17,18] which were designed for the treatment of Fe overload disease (Figure 4A). These results suggest that the HMPIH series are better able to gain access to and mobilize intracellular Fe pools through their increased lipophilicity. This was particularly obvious in the case of HMPAH and HMPHH, which demonstrated 34 ± 1% and 39 ± 1% of cellular ^{59}Fe release, respectively, while the ^{59}Fe mobilizing efficacy of their more hydrophilic analogs, HPCAH and HPCHH, were comparable to that of the control medium (Figure 4A). These results for the latter two HPCIH analogs agree with our previous studies.[17] In addition, HMP3BBH and HMP4BBH showed significantly ($p < 0.01$) increased levels of ^{59}Fe mobilization in comparison to their analogous and more cytotoxic HPKIH counterparts. This fact again confirms the hypothesis that Fe chelation efficacy is not directly proportional to antiproliferative activity.[36] Indeed, other factors must be considered such as the redox activity of the resultant Fe complexes of the chelators and their relative abilities to target different Fe pools within the cell.[30]

In summary, all members of the HMPIH series, particularly HMPIH and HMPTH, demonstrated high levels of cellular ^{59}Fe release and, thus, are potential agents for the treatment of Fe overload disorders.

Inhibition of Cellular ^{59}Fe Uptake from ^{59}Fe-Transferrin. Another important factor to consider regarding the suitability of the HMPIH series as potential agents for the treatment of Fe overload disease was their ability to prevent Fe uptake from the Fe transport protein, transferrin (Fe-Tf).[17] The ability of the HMPIH series to inhibit uptake of ^{59}Fe from ^{59}Fe-Tf in SK-N-MC neuroepithelioma cells was examined in comparison to their HPCIH and HPKIH counterparts, and the controls, H$_2$PIH, H$_2$NIH, and DFO (Figure 4B). As previously demonstrated,[17,21,32] the positive controls, H$_2$PIH and H$_2$NIH, were very effective at
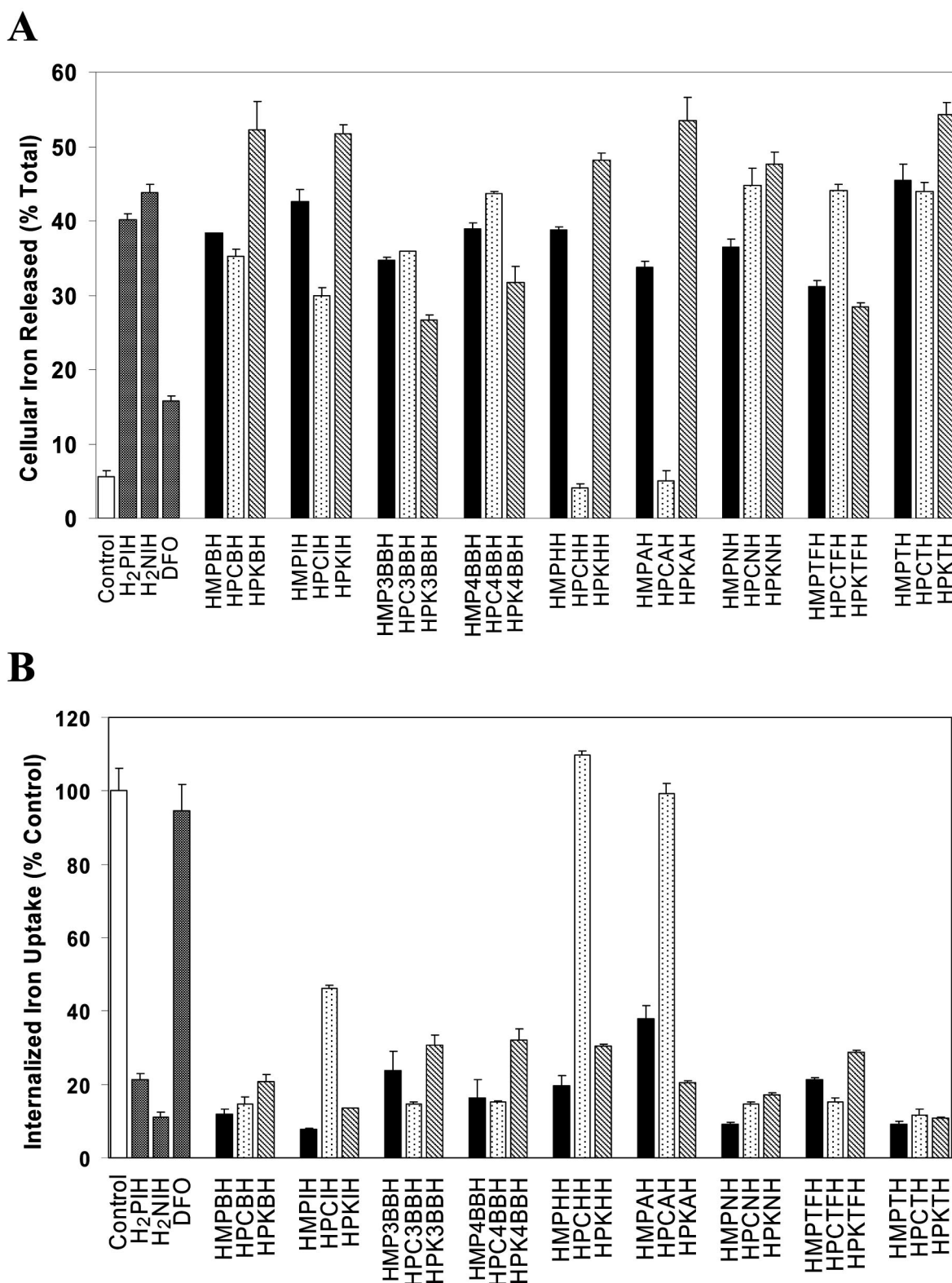
Figure 4. The effect of the HMPIH series in comparison with their HPCIH and HPKIH analogs on (A) ^{59}Fe mobilization from prelabeled SK-N-MC neuroepithelioma cells and (B) ^{59}Fe uptake from ^{59}Fe-transferrin (^{59}Fe-Tf) by SK-N-MC neuroepithelioma cells. Results are mean $\pm$ SD of three experiments with three determinations in each experiment.

inhibiting ^{59}Fe uptake from ^{59}Fe-Tf, reducing it to 21% and 11% of the control, respectively (Figure 4B). In comparison, DFO showed poor ability to inhibit ^{59}Fe uptake, as previously demonstrated,[17,21,32] reducing ^{59}Fe uptake to 94 $\pm$ 7% of control (Figure 4B).

Importantly, the HMPIH series effectively inhibited the uptake of ^{59}Fe from ^{59}Fe-Tf to 8–38% of the untreated control (Figure 4B). Those chelators that mediated high levels of cellular ^{59}Fe efflux also markedly inhibited ^{59}Fe uptake, which included HMPIH, HMPNH, and HMPTH (Figure 4B). As observed in

Table 4. Effect of the HMPIH, HPCIH, and HPKIH Series at Inhibiting the Growth of the SK-N-MC Neuroepithelioma Cell Line; Comparable Data for DFO, 3-AP, H_2NIH, and HDp44mT are Also Shown[a]

ligand	IC$_{50}$ (μM)	ligand	IC$_{50}$ (μM)	ligand	IC$_{50}$ (μM)
DFO	12.05 ± 0.09				
3-AP	0.66 ± 0.09				
H$_2$NIH	0.83 ± 0.36				
HDp44mT	0.001 ± 0.001				
HMPIH	5.79 ± 1.00	HPCIH	>80	HPKIH	0.83 ± 0.14
HMPBH	3.62 ± 0.71	HPCBH	19.20 ± 0.68	HPKBH	3.04 ± 0.28
HMP3BBH	1.15 ± 0.32	HPC3BBH	13.54 ± 2.25	HPK3BBH	0.24 ± 0.04
HMP4BBH	1.22 ± 0.10	HPC4BBH	17.66 ± 0.49	HPK4BBH	0.30 ± 0.02
HMPHH	16.76 ± 1.52	HPCHH	>80	HPKHH	7.53 ± 0.07
HMPAH	58.78 ± 3.71	HPCAH	>80	HPKAH	7.64 ± 0.68
HMPTFH	1.16 ± 0.15	HPCTFH	22.39 ± 3.81	HPKTFH	0.24 ± 0.02
HMPNH	1.39 ± 0.01	HPCNH	35.50 ± 3.91	HPKNH	0.26 ± 0.02
HMPTH	2.13 ± 0.04	HPCTH	22.66 ± 3.91	HPKTH	0.95 ± 0.17

[a] Results are expressed as the mean ± SD (three experiments).

the efflux study, no correlation was evident between the log P values of the HMPIH series and their ability to prevent the uptake of ^{59}Fe from Tf. All members of the HMPIH series, except HMPAH, showed significantly ($p < 0.01$) higher or comparable levels of ^{59}Fe uptake inhibition to that of the positive control, H$_2$PIH. The ligands, HMPIH, HMPBH, HMPNH, and HMPTH, exhibited significantly ($p < 0.05$) higher or comparable inhibition of ^{59}Fe uptake from ^{59}Fe-Tf to that of H$_2$NIH. DFO was significantly ($p < 0.001$) less effective at preventing ^{59}Fe uptake from ^{59}Fe-Tf than all HMPIH members (Figure 4B).

All members of the HMPIH series, except HMP3BBH and HMPTFH, were significantly ($p < 0.001$) more effective or had comparable activity to that of their HPCIH counterparts at preventing ^{59}Fe uptake from ^{59}Fe-Tf (Figure 4B). As observed in the Fe efflux study, both HMPHH and HMPAH were significantly ($p < 0.001$) more efficient than their more hydrophilic HPCHH and HPCAH analogues. Also, all HMPIH analogs, besides HMPAH, were significantly ($p < 0.005$) more effective or comparable to that of their analogous HPKIH homologue at inhibiting ^{59}Fe uptake (Figure 4B). These results highlight the high Fe mobilizing efficacy of the HMPIH series and emphasize their potential to treat Fe overload disease.

Antiproliferative Activity of the Ligands against Tumor Cells. Although Fe chelators can be used for the treatment of Fe overload disease, they can also be designed to act as antiproliferative agents.[21–23,31–33] For an Fe chelator to be a potential candidate for the treatment of Fe overload disorders, it must be able to effectively chelate intracellular Fe without inducing toxic effects. Thus, it was important to determine the antiproliferative effects of the HMPIH analogs. This was performed using SK-N-MC neuroepithelioma cells, as the effects of Fe chelators on their growth have been extensively examined.[21,33,35,39,41] The novel HMPIH series were compared to a number of controls, including (1) their corresponding HPCIH and HPKIH analogs,[17,22,23] (2) DFO, (3) 3-aminopyridine-2-carboxaldehyde thiosemicarbazone (3-AP; Figure 1A), a chelator designed specifically as a chemotherapeutic agent,[42,43] (4) H$_2$NIH,[44] and (5) di-2-pyridylketone 4,4-dimethyl-3-thiosemicarbazone (HDp44mT; Figure 1A), a ligand with potent antiproliferative activity.[31,33] As previously determined,[21,31–33] 3-AP (IC$_{50}$ 0.66 ± 0.09 μM; Table 4) and H$_2$NIH (IC$_{50}$ 0.83 ± 0.36 μM; Table 4) showed moderate antiproliferative effects, while HDp44mT (IC$_{50}$ 0.001 ± 0.001 μM; Table 4) demonstrated potent antiproliferative activity. In contrast, the hydrophilic chelator, DFO (IC$_{50}$ 12.05 ± 0.09 μM; Table 4), showed poor antitumor effects, as previously observed.[21,22,32,33]

The HMPIH series was found to have only modest to limited antiproliferative activity (IC$_{50}$ 1.15–58.78 μM; Table 4), with

no correlation between the log P value and the antiproliferative activity observed. The majority of the HMPIH members showed significantly ($p < 0.05$) lower antiproliferative effects than the controls, 3-AP, H$_2$NIH, and HDp44mT. Only HMPAH and HMPHH were found to have significantly ($p < 0.01$) lower antiproliferative activity than DFO. Notably, both these latter analogs were significantly more effective than DFO at mobilizing intracellular ^{59}Fe and preventing ^{59}Fe uptake from ^{59}Fe-Tf. Such properties are important for considering these chelators as new agents for the treatment of Fe overload disease.

All HMPIH analogs showed significantly ($p < 0.001$) higher antiproliferative activity than their corresponding HPCIH counterparts (Table 4) but were significantly ($p < 0.05$) less cytotoxic than their HPKIH analogs (Table 4). As discussed previously, lipophilicity of aroylhydrazone ligands plays an important role in their antiproliferative activity.[21] While there was no correlation between log P values of the individual HMPIH series ligands and their antiproliferative activity, their general increase in lipophilicity (due to the methyl group) relative to their HPCIH counterparts (Figure 1B) could be responsible for this effect. In terms of the higher antiproliferative effects of the HPKIH analogs, their higher lipophilicity than the analogous HPCIH and HMPIH chelators together with their redox activity are crucial factors to consider.[22–24]

These results illustrate the modest antitumor effects of the HMPIH series of chelators, suggesting the potential of some of these agents for the treatment of Fe overload.

Antiproliferative Activity of the Fe Complexes against Tumor Cells. Previous studies have demonstrated that some Fe complexes demonstrate increased antiproliferative activity relative to their free ligands.[39,45–47] Hence, we examined the antitumor activity of the synthesized Fe^{II}-MPIH series complexes on SK-N-MC neuroepithelioma cells (Table 5).

The majority of Fe^{II} complexes of the HMPIH series demonstrated significantly ($p < 0.05$) lower antiproliferative effects in comparison to that of their free ligands (Table 5). In fact, the Fe complexes resulted in a 2- to 23-fold decrease in antiproliferative activity. This reduced activity of these complexes to inhibit growth can be attributed to their inability to complex intracellular Fe that is necessary for essential metabolic processes.

Only the Fe^{II} complex of HMP3BBH showed comparable antitumor activity to that of the free ligand (Table 5). Of interest, the Fe^{II} complexes of the ligands, HMPHH and HMPAH, showed the lowest antiproliferative activity (IC$_{50}$ values 55.35 and >80 μM, respectively) of all the HMPIH series, again illustrating the potential of these agents for the treatment of Fe overload.

Table 5. Effect of the HMPIH Series and their Fe[II] Complexes at Inhibiting the Growth of the SK-N-MC Neuroepithelioma and Normal MCR-5 Fibroblast Cell Lines[a]

ligand	IC$_{50}$ (μM) of ligand against SK-N-MC cells	IC$_{50}$ (μM) of Fe[II](L)$_2$ complex against SK-N-MC cells	*p* value (ligand vs Fe[II] complex)	IC$_{50}$ (μM) of ligand against MRC-5 fibroblast cells	*p* value (SK-N-MC vs MRC-5 cells)
HMPIH	5.79 ± 1.00	23.17 ± 4.49	*p* < 0.005	25.20 ± 9.81	*p* < 0.05
HMPBH	3.62 ± 0.71	48.88 ± 12.43	*p* < 0.005	7.04 ± 1.01	*p* < 0.01
HMP3BBH	1.15 ± 0.32	1.61 ± 0.29	*p* > 0.05	3.12 ± 0.27	*p* < 0.001
HMP4BBH	1.22 ± 0.10	27.90 ± 1.46	*p* < 0.001	2.94 ± 0.71	*p* < 0.01
HMPHH	16.76 ± 1.52	55.35 ± 18.40	*p* < 0.05	>80	*p* < 0.001
HMPAH	58.78 ± 3.71	>80	*p* < 0.001	>80	*p* < 0.001
HMPTFH	1.16 ± 0.15	9.09 ± 0.59	*p* < 0.001	2.09 ± 0.61	*p* > 0.05
HMPNH	1.39 ± 0.01	2.71 ± 0.29	*p* < 0.005	2.87 ± 0.25	*p* < 0.001
HMPTH	2.13 ± 0.04	26.61 ± 5.38	*p* < 0.001	5.54 ± 0.89	*p* < 0.005

[a] The *p* values were determined using Student's *t*-test and compare the antiproliferative activity of the HMPIH series in SK-N-MC cells against their Fe complex or the HMPIH series in SK-N-MC cells against MRC-5 cells. Results are expressed as the mean ± SD (three experiments).

Antiproliferative Activity of the Ligands against Normal Cells. For an Fe chelator to be considered as a therapeutic agent for the treatment of Fe overload disorders, it must have high Fe mobilization efficacy without exhibiting toxic effects to normal cells. Therefore, the antiproliferative activity of the HMPIH series of ligands was also assessed in the mortal MRC-5 fibroblast cell line (Table 5).

The HMPIH series demonstrated moderate to poor antiproliferative activity against mortal MRC5 fibroblasts (IC$_{50}$ 2.09 to >80 μM; Table 5). Those analogs that exhibited effective Fe chelation activity (Figure 4A,B) and low antiproliferative activity against SK-N-MC tumor cells, such as HMPHH and HMPAH, also had minimal antiproliferative effects against fibroblasts (IC$_{50}$ values >80 μM; Table 5). The majority of the HMPIH series demonstrated significantly (*p* < 0.05) decreased antiproliferative effects in fibroblasts when compared to the antitumor activity observed in SK-N-MC cells (Table 5). In fact, a 2- to 5-fold decrease in antiproliferative activity was observed. Only the antiproliferative activity of HMPTFH showed no significant difference between the neoplastic and the normal cell types. These results demonstrating the low antiproliferative effects of the HMPIH analogs (particularly HMPHH and HMPAH) on mortal cells makes them potentially suitable for the treatment of Fe overload disease.

Ascorbate Oxidation by the Fe Complexes. Many Fe chelators are known to form redox-active Fe complexes, which produce harmful ROS, initiating cellular damage.[23,31,32,48] Therefore, it was essential to determine the redox activity of the Fe complexes of the HMPIH series. This was particularly important considering the potential of several of these chelators for the treatment of Fe overload. Considering this, we examined the ability of the HMPIH-Fe complexes to mediate the oxidation of the physiological substrate, ascorbate, using established methodology.[23,31,32] Ascorbate oxidation mediated by the HMPIH Fe complexes was compared to their related HPCIH and HPKIH analogs (Figure 5). In addition, ascorbate oxidation by the positive control, EDTA, was also assessed.[23,31,32]

The results of these experiments were expressed in terms of iron-binding equivalents (IBE) due to the varying denticity of the chelators examined. For example, the hexadentate EDTA ligand forms a 1:1 Fe/ligand complex, while the tridentate ligands of the HMPIH, HPCIH, and HPKIH series, form 1:2 Fe/ligand complexes.[23,49] Three IBEs were chosen, 0.1, 1, and 3, to examine the redox activity of these aroylhydrazones. An IBE of 0.1 represents an excess of Fe, where one hexadentate or two tridentate ligands are in the presence of 10 Fe atoms. An IBE of 1 results in complete filling of the coordination sphere, while an IBE of 3 represents an excess of the ligand, where three hexadentate or six tridentate ligands are in the presence of one Fe ion.

As previously determined,[23,24,31,32,48,50] the Fe−EDTA complex was highly redox active and increased ascorbate oxidation to 320 and 323% of the control at an IBE of 1 and 3, respectively (Figure 5). In addition, EDTA was significantly (*p* < 0.001) more effective at increasing ascorbate oxidation than all members of the HMPIH series at all IBEs. In contrast to EDTA, the HMPIH series prevented ascorbate oxidation, reducing it to 71–97, 48–92, and 25–102% of the control at an IBE of 0.1, 1, and 3, respectively (Figure 5). It is of interest to note that the majority of the HMPIH series demonstrated comparable or significantly (*p* < 0.05) reduced levels of ascorbate oxidation to that of their HPCIH and HPKIH counterparts at all IBEs (Figure 5). It was demonstrated in our previous studies that the Fe complexes of the majority of the HPKIH series mediated protective or comparable levels of ascorbate oxidation to that of the control.[23] The greater protective effects of the HMPIH series on ascorbate oxidation in comparison to their HPKIH analogs may be attributed to the slightly increased redox potentials of their Fe[II] complexes. Cumulatively, these results emphasize the suitability of the HMPIH series as agents for the treatment of Fe overload disease.

Benzoate Hydroxylation. As an additional measurement of redox activity, we assessed the ability of the Fe complexes of the HMPIH series to mediate benzoate hydroxylation (Figure 6). Again, these assays were done in comparison to analogous HPCIH and HPKIH chelators. The benzoate hydroxylation assay measures the activity of the Fe complexes to catalyze the breakdown of hydrogen peroxide, generating hydroxyl radicals that subsequently hydroxylate benzoate.[31,32,48]

In the presence of Fe[II], the positive control, EDTA, enhanced benzoate hydroxylation to 182 and 229% of the control at IBEs of 1 and 3, respectively (Figure 6). This was in agreement with previous studies.[31,48] As observed with the ascorbate oxidation assay, EDTA significantly (*p* < 0.01) increased benzoate hydroxylation to a greater level than the HMPIH series analogs at all IBEs (Figure 6).

As demonstrated in the ascorbate oxidation assay, all Fe complexes of the HMPIH series showed protective effects, reducing benzoate hydroxylation to 46–56, 23–84, and 27–106% of the control at IBEs of 0.1, 1, and 3, respectively (Figure 6). Importantly, the Fe complexes of the HMPIH series were found to mediate comparable or significantly (*p* < 0.05) reduced levels of benzoate hydroxylation than their corresponding HPCIH and HPKIH analogs at all IBEs. As previously observed, the majority of HPKIH chelators were able to increase benzoate hydroxylation.[23] Again, the increased protective effects of the Fe complexes of the HMPIH series at preventing benzoate hydroxylation can be attributed to their irreversible electrochemistry and increased redox potentials in comparison to the HPKIH Fe complexes. These results suggest the HMPIH series Fe
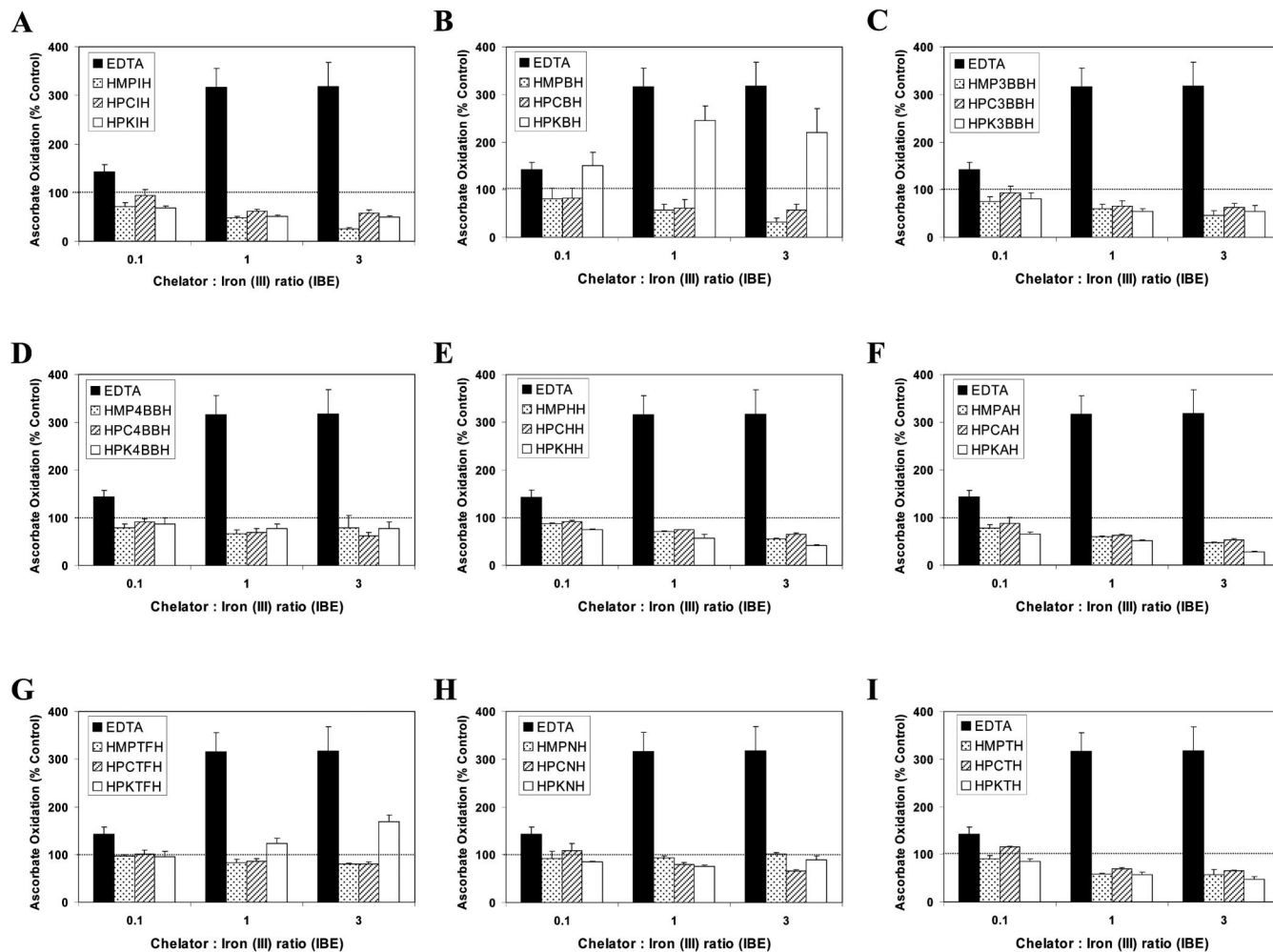
Figure 5. Effect of the Fe complexes of the HMPIH series and their corresponding HPCIH and HPKIH analogs on ascorbate oxidation. Chelators at iron-binding equivalent (IBE) ratios of 0.1, 1, and 3 were incubated in the presence of Fe^{III} (10 μM) and ascorbate (100 μM). The UV absorbance at 265 nm was recorded after 10 and 40 min and the difference between the time points was calculated. Comparison of the positive control EDTA with the following: (A) HMPIH, HPCIH and HPKIH; (B) HMPBH, HPCBH, and HPKBH; (C) HMP3BBH, HPC3BBH, and HPK3BBH; (D) HMP4BBH, HPC4BBH, and HPK4BBH; (E) HMPHH, HPCHH, and HPKHH; (F) HMPAH, HPCAH, and HPKAH; (G) HMPTFH, HPCTFH, and HPKTFH; (H) HMPNH, HPCNH, and HPKNH; and (I) HMPTH, HPCTH, and HPKTH. Results are mean ± SD (three experiments).

complexes are redox inactive, binding Fe and preventing ROS generation. This is an important property of Fe chelators suitable for the treatment of Fe overload.

Conclusions

The design and synthesis of novel orally active Fe chelators with high Fe mobilization efficacy and low toxicity remains an ongoing priority in the treatment of Fe overload disease. We designed and synthesized the novel HMPIH series of ligands, which demonstrate high Fe chelation efficacy. In fact, the majority of the HMPIH ligands showed comparable or significantly ($p < 0.005$) greater activity than their HPCIH analogs at mobilizing cellular ^{59}Fe or preventing ^{59}Fe uptake from ^{59}Fe-Tf. Of note, HMPHH and HMPAH showed high Fe chelation efficacy that was significantly greater than DFO and also very low antiproliferative activity against normal cells, two crucial properties essential for the development of chelators for the treatment of Fe overload.

An interesting difference between the HMPIH analogs that are Fe^{II} chelators and the chelators currently used for the treatment of Fe overload (i.e., DFO, deferiprone, and 4-[3,5-bis(2-hydroxyphenyl)-1,2,4-triazol-1-yl]benzoic acid) is that the latter are Fe^{III}-binding ligands.[5] Considering this and the mechanism of Fe chelation of the HMPIH series, it is well-

known that both redox states exist in equilibrium within cells.[51] Because Tf binds Fe^{III}, clearly the HMPIH ligands cannot remove Fe from this protein directly but can probably intercept it after its reduction within the endosome during receptor-mediated endocytosis.[52] The Fe^{II} is transported through the endosomal membrane by the divalent metal transporter 1[53] and enters the labile iron pool where it can be used for metabolic processes.[5] Our ^{59}Fe uptake studies demonstrate that this Fe^{II} in transit can be intercepted by the HMPIH analogs to form a neutral Fe^{II} complex that then readily diffuses out of the cell. It is of interest to note that in the current study, the Fe^{III} complexes of HMPIH series ligands could not be isolated despite repeated attempts. This is probably due to the *N,N,O*-donor atoms that lead to a preference for the Fe^{II} state.

The results of the ascorbate oxidation and benzoate hydroxylation assays suggested that the HMPIH series of ligands bind Fe and prevent it from redox cycling. This was in agreement with studies assessing the Fe complexes of these ligands, which showed their irreversible electrochemistry in the presence of water.

Comparison of the electrochemical data of the HMPIH Fe complexes with that of closely related ligands[27] highlighted the important role of the additional electron-withdrawing pyrazine N-atom in the irreversible redox chemistry of the HMPIH-Fe
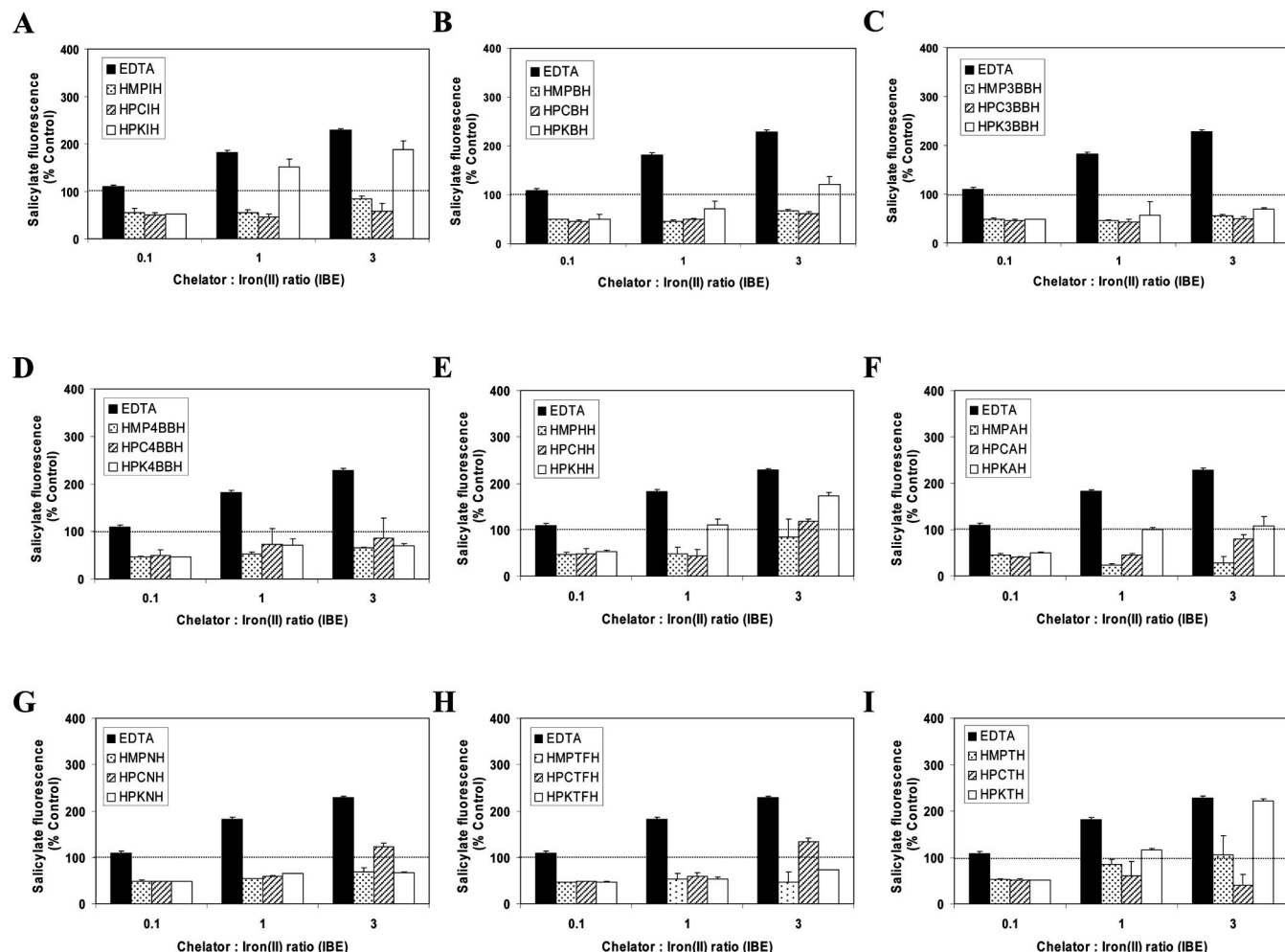
Figure 6. The effect of various Fe chelators on the hydroxylation of benzoate in the presence of Fe^{II} and hydrogen peroxide. Chelators at iron-binding equivalent (IBE) ratios of 0.1, 1, and 3 were incubated for 1 h at room temperature in the presence of Fe^{II} (30 μM), hydrogen peroxide (5 mM), and benzoate (1 mM). The fluorescence of hydroxylated benzoate was measured at 308 nm excitation and 410 nm emission. Comparison of the positive control EDTA with (A) HMPIH, HPCIH, and HPKIH, (B) HMPBH, HPCBH, and HPKBH, (C) HMP3BBH, HPC3BBH, and HPK3BBH, (D) HMP4BBH, HPC4BBH, and HPK4BBH, (E) HMPHH, HPCHH, and HPKHH, (F) HMPAH, HPCAH, and HPKAH, (G) HMPTFH, HPCTFH, and HPKTFH, (H) HMPNH, HPCNH, and HPKNH, and (I) HMPTH, HPCTH, and HPKTH. Results are mean $\pm$ SD (three experiments).

complexes. This critical structure–activity relationship underlined the significance of electron-withdrawing groups in the generation of novel *N,N,O* aroylhydrazones that form Fe complexes with limited redox and antiproliferative activity. The prevention of ROS generation is an important factor that needs to be taken into account when designing novel ligands for the treatment of Fe overload disease.

Collectively, the chemical properties and biological activity of the HMPIH analogs, in particular, HMPHH and HMPAH, make them suitable agents for the treatment of Fe overload.

Experimental Section

Synthesis. All commercial reagents were used without further purification. Desferrioxamine (DFO) was purchased from Novartis, Basel, Switzerland. 3-AP was a gift from Vion Pharmaceuticals, New Haven, CT. The HPCIH and HPKIH series analogs, H$_2$NIH, H$_2$PIH, and HDp44mT were prepared using standard procedures.[17,37,54,55]

Physical Methods. ^{1}H NMR (300 MHz) spectra of the free ligands were acquired in the specified solvents on a Varian Gemini 300 BB NMR spectrometer. ^{1}H NMR (400 MHz) spectra of the complexes were acquired on a Bruker AV400 spectrometer, in d_6-DMSO, with an external reference capillary containing d_6-DMSO and TMS. Infrared spectra were measured on a Bruker FT-IR IFS 66V spectrophotometer using an ATR (attenuated total reflectance) assembly. ESI mass spectra were obtained on a ThermoFinnigan

TSQ 7000 spectrometer. Elemental analysis was conducted using a Carlo Erba 1106 analyzer. Cyclic voltammetry was performed using a BAS100B/W potentiostat. For the mixed solvent aqueous electrochemistry, a glassy carbon working electrode, an aqueous Ag/AgCl reference, and Pt wire auxiliary electrode were used. All complexes were measured as saturated solutions (<1 mM) in DMF/H$_2$O 70:30 v/v. The supporting electrolyte was NaClO$_4$ (0.1 M) and the solutions were purged with nitrogen prior to measurement. All potentials are cited versus the normal hydrogen electrode (NHE) by addition of 196 mV to the potentials measured relative to the Ag/AgCl reference. Nonaqueous electrochemistry was performed using DMF containing 0.1 M Et$_4$NClO$_4$ as the supporting electrolyte. A nonaqueous reference electrode was used and cyclic voltammograms were referenced to the ferrocene couple. Due to the low solubility of the complexes, electrochemistry was run using saturated solutions. UV–vis measurements were made in acetonitrile. Due to low solubility, solutions of Fe(MPAH)$_2$, Fe(MPTH)$_2$, and Fe(MP4BBH)$_2$ were filtered immediately prior to measurement. The concentration of the complexes was determined by taking a known volume of the acetonitrile solution, evaporating to dryness under vacuum, and diluting to a known volume with dilute nitric acid. The Fe concentrations of the HMPTH and HMP4BBH samples were determined by AAS (Varian SpectrAA 220FS Atomic Absorption Spectrometer, 248.3 nm). The Fe concentration of the HMPAH sample was determined by inductively coupled plasma mass spectrometry (Analytical Services Unit, School of Land and

Food Sciences, University of Queensland). Octanol–water partition coefficients were measured spectrophotometrically, as described elsewhere.[28]

Elemental analysis (C, H, N) of the ligands and complexes was performed, and the results, available as Supporting Information, were within ±0.4% of the theoretical values, unless otherwise stated.

Crystallography. Cell constants at 293 K were determined by a least-squares fit to the setting parameters of 25 independent reflections measured on an Enraf-Nonius CAD4 four-circle diffractometer employing graphite-monochromated Mo Kα radiation (0.71073 Å) and operating in the ω-2θ scan mode within the range 2 < 2θ < 50 Å. Data reduction was performed with the WINGX suite of programs.[56] Structures were solved by direct methods with SHELXS and refined by full-matrix least-squares analysis with SHELXL-97.[57] All non-H atoms were refined with anisotropic thermal parameters. Aryl H-atoms were included at estimated positions using a riding model. Amide H-atoms were first located from difference maps then restrained at these positions in a similar manner to that employed for the remaining H-atoms. Molecular structure diagrams were produced with ORTEP3.[58] The data in CIF format has been deposited at the Cambridge Crystallographic Data Centre.

Methyl Pyrazinylketone Benzoyl Hydrazone (HMPBH). Equimolar amounts of acetyl pyrazine (0.50 g, 4.1 mmol) and benzoic acid hydrazide (0.56 g, 4.1 mmol) were dissolved in ethanol (70 mL) with stirring. A few drops of concentrated HCl were added as a catalyst. The reaction solution was refluxed for 5 h and the crystallized product was collected by vacuum filtration, washed with cold ethanol, and air-dried. This afforded HMPBH (60%) as long, pale yellow crystals: Anal. ($C_{13}H_{12}N_4O$) C, H, N; IR (cm^{-1}) 3376 (m), 3046 (w), 1682 (s), 1599 (m), 1578 (m), 1533 (s), 1514 (s), 1490 (m), 1467 (m), 1323 (m), 1253 (s), 1172 (m), 1073 (m), 1015 (m), 903 (m), 841 (m), 801 (m), 710 (s), 686 (s), 656 (m), 579 (w); ^{1}H NMR (d_6-DMSO) δ 11.09 (s, 1H, NH), 9.27 (s, 1H, ArH), 8.67 (m, 2H, ArH), 7.90 (d, 2H, ArH), 7.65 − 7.52 (m, 3H, ArH), 2.47 (s, 3H, CH$_3$); MS (ESI) m/z 241 (M + H$^+$), 263 (M + Na$^+$). Single crystals suitable for X-ray crystallography were grown by slow evaporation of an ethanol solution. All other members of the HMPIH series were prepared in a similar manner.

Methyl Pyrazinylketone Isonicotinoyl Hydrazone (HMPIH). HMPIH (73%) was collected as a fibrous white solid: Anal. ($C_{12}H_{11}N_5O$) C, H, N; IR (cm^{-1}) 3182 (m), 3046 (w), 1669 (s), 1617 (w), 1597 (w), 1554 (w), 1501 (w), 1459 (w), 1418 (w), 1381 (m), 1304 (m), 1225 (w), 1169 (m), 1126 (w), 1099 (w), 1010 (w), 863 (w), 841 (m), 803 (w), 753 (m), 724 (m), 687 (w), 631 (w), 585 (w); ^{1}H NMR (d_6-DMSO) δ 11.39 (s, 1H, NH), 9.29 (s, 1H, ArH), 8.80 (d, 2H, ArH), 8.70 (m, 2H, ArH), 7.84 (d, 2H, ArH), 2.48 (s, 3H, CH$_3$); MS (ESI) m/z 242 (M + H$^+$).

Methyl Pyrazinylketone *m*-Bromobenzoyl Hydrazone (HMP3BBH). HMP3BBH (59%) was collected as a fibrous white solid: Anal. ($C_{13}H_{11}N_4OBr$) C, H, N IR (cm^{-1}) 3191 (m), 1667 (s), 1617 (w), 1560 (w), 1523 (w), 1467 (w), 1364 (m), 1303 (w), 1173 (w), 1157 (w), 1126 (w), 1104 (w), 1067 (w), 1049 (w), 1010 (w), 885 (w), 852 (w), 819 (w), 801 (m), 741 (m), 714 (m), 694 (w), 678 (w), 631 (w); ^{1}H NMR (d_6-DMSO) δ 11.20 (s, 1H, NH), 9.28 (s, 1H, ArH), 8.68 (m, 2H, ArH), 8.09 (s, 1H, ArH), 7.91 (d, 1H, ArH), 7.82 (d, 1H, ArH), 7.52 (dd, 1H, ArH), 2.47 (s, 3H, CH$_3$); MS (ESI) m/z 319 (M + H$^+$), 321 (M + H$^+$), 341 (M + Na$^+$), 343 (M + Na$^+$).

Methyl Pyrazinylketone *p*-Bromobenzoyl Hydrazone (HMP4BBH). HMP4BBH (74%) was collected as yellow needles: Anal. ($C_{13}H_{11}N_4OBr$) C, H, N; IR (cm^{-1}) 3188 (w), 3074 (w), 2950 (w), 1681 (s), 1582 (m), 1560 (w), 1483 (w), 1460 (m), 1397 (m), 1363 (m), 1302 (m), 1178 (m), 1121 (w), 1091 (w), 1071 (w), 1049 (w), 1011 (m), 848 (m), 806 (w), 772 (w), 741 (m), 710 (w), 647 (w), 565 (w); ^{1}H NMR (d_6-DMSO) δ 11.16 (s, 1H, NH), 9.27 (s, 1H, ArH), 8.68 (m, 2H, ArH), 7.85 (d, 2H, ArH), 7.75 (d, 2H, ArH), 2.46 (s, 3H, CH$_3$); MS (ESI) m/z 319 (M + H$^+$), 321 (M + H$^+$), 341 (M + Na$^+$), 343 (M + Na$^+$).

Methyl Pyrazinylketone *p*-Hydroxybenzoyl Hydrazone (HMPHH). HMPHH (80%) was collected as small yellow crystals: Anal. ($C_{13}H_{12}N_4O_2$) C, H, N; IR (cm^{-1}) 3296 (m), 1652 (s), 1607

(m), 1581 (m), 1540 (m), 1508 (m), 1465 (w), 1319 (w), 1259 (s), 1015 (m), 903 (w), 845 (m), 757 (m), 701 (m), 616 (m), 579 (w); ^{1}H NMR (d_6-DMSO) δ 10.82 (s, 1H, NH), 10.18 (s, 1H, OH), 9.21 (s, 1H, ArH), 8.67 (dd, 1H, ArH), 8.64 (d, 1H, ArH), 7.82 (d, 2H, ArH), 6.90 (d, 2H, ArH), 2.45 (s, 3H, CH$_3$); MS (ESI) m/z 257 (M + H$^+$), 279 (M + Na$^+$). Single crystals suitable for X-ray analysis were grown by slow evaporation of an ethanol solution.

Methyl Pyrazinylketone *p*-Aminobenzoyl Hydrazone (HMPAH). HMPAH (66%) was collected as small white crystals: Anal. ($C_{13}H_{13}N_5O$) C, H, N; IR (cm^{-1}) 3444 (m), 3352 (m), 3234 (m), 1655 (s), 1603 (s), 1502 (s), 1257 (s), 1195 (w), 1134 (w), 835 (m), 756 (m), 694 (w), 616 (m); ^{1}H NMR (d_6-DMSO) δ 10.50 (s, 1H, NH), 9.18 (d, 1H, ArH), 8.62 (dd, 1H, ArH), 8.59 (d, 1H, ArH), 7.66 (d, 2H, ArH), 6.59 (d, 2H, ArH), 2.40 (s, 3H, CH$_3$); MS (ESI) m/z 256 (M + H$^+$), 278 (M + Na$^+$).

Methyl Pyrazinylketone *p*-Trifluoromethylbenzoyl Hydrazone (HMPTFH). HMPTFH (78%) was collected as thick white crystals: Anal. ($C_{14}H_{11}N_4OF_3$) C, H, N; IR (cm^{-1}) 3336 (s), 3058 (w), 1675 (s), 1580 (m), 1531 (s), 1510 (w), 1467 (m), 1439 (m), 1407 (m), 1367 (m), 1329 (s), 1267 (m), 1011 (m), 903 (m), 863 (m), 768 (m), 708 (m), 689 (m), 667 (w), 593 (w), 548 (w); ^{1}H NMR (d_6-DMSO) δ 11.32 (s, 1H, NH), 9.30 (s, 1H, ArH), 8.69 (m, 2H, ArH), 8.11 (d, 2H, ArH), 7.92 (d, 2H, ArH), 2.48 (s, 3H, CH$_3$); MS (ESI) m/z 309 (M + H$^+$). Single crystals suitable for X-ray analysis were grown by slow evaporation of an ethanol solution.

Methyl Pyrazinylketone *p*-Nitrobenzoyl Hydrazone (HMPNH). HMPNH (77%) was collected as fine yellow needles: Anal. ($C_{13}H_{12}N_4O_3$) C, H, N; IR (cm^{-1}) 3176 (m), 3046 (w), 1666 (s), 1599 (m), 1516 (s), 1458 (w), 1349 (s), 1270 (m), 1150 (w), 1008 (w), 844 (m), 687 (m); ^{1}H NMR (d_6-DMSO) δ 11.41 (s, 1H, NH), 9.29 (s, 1H, ArH), 8.68 (m, 2H, ArH), 8.37 (d, 2H, ArH), 8.16 (d, 2H, ArH), 2.48 (s, 3H, CH$_3$); MS (ESI) m/z 286 (M + H$^+$), 308 (M + Na$^+$).

Methyl Pyrazinylketone 2-Thiophenecarboxyl Hydrazone (HMPTH). HMPTH (77%) was collected as fine white needles: Anal. ($C_{11}H_{10}N_4OS$) C, H, N; IR (cm^{-1}) 3166 (m), 3048 (w), 1645 (s), 1599 (w), 1516 (m), 1420 (w), 1382 (w), 1338 (w), 1300 (w), 1222 (w), 1176 (w), 1122 (w), 1093 (w), 1047 (w), 1031 (w), 1011 (w), 854 (w), 808 (w), 744 (w), 723 (m), 704 (m), 639 (w), 549 (w), 474 (w), 464 (m), 420 (w); ^{1}H NMR (d_6-DMSO) δ 11.22 (s, 1H, NH), 9.36 (s, 1H, ArH), 8.69 (dd, 1H, ArH), 8.66 (d, 1H, ArH), 8.08 (dd, 1H, ArH), 8.00 (d, 1H, ArH), 7.25 (dd, 1H, ArH), 2.45 (s, 3H, CH$_3$); MS (ESI) m/z 269 (M + Na$^+$).

2-Pyridylcarboxaldehyde *p*-Trifluoromethylbenzoyl Hydrazone (HPCTFH). Equimolar amounts of 2-pyridylcarboxaldehyde (0.40 g, 3.7 mmol) and *p*-trifluoromethylbenzoic acid hydrazide (0.76 g, 3.7 mmol) were dissolved in ethanol (70 mL) with stirring. A few drops of concentrated HCl were added as catalyst. The reaction solution was refluxed for 5 h and the product was collected by vacuum filtration, washed with cold ethanol, and air-dried. HPCTFH (54%) was collected as thin white needles: Anal. ($C_{14}H_{10}N_3OF_3$) C, H, N; IR (cm^{-1}) 3165 (m), 3042 (w), 1647 (s), 1583 (m), 1551 (m), 1466 (w), 1437 (w), 1409 (w), 1328 (m), 1302 (w), 1284 (m), 1167 (w), 1146 (w), 1119 (m), 1062 (w), 1018 (w), 992 (w), 953 (w), 919 (w), 857 (w), 775 (w), 749 (w), 687 (w), 618 (w); ^{1}H NMR (d_6-DMSO) δ 12.27 (s, 1H, NH), 8.66 (dd, 1H, ArH), 8.52 (s, 1H, HC=N), 8.16 (d, 2H, ArH), 8.02 (d, 1H, ArH), 7.99 (m, 3H, ArH), 7.47 (ddd, 1H, ArH); MS (ESI) m/z 294 (M + H$^+$), 316 (M + Na$^+$). All additional HPCIH analogs were prepared in a similar manner.

2-Pyridylcarboxaldehyde *p*-Nitrobenzoyl Hydrazone (HPCNH). HPCNH (53%) was collected as small yellow crystals: Anal. ($C_{13}H_{10}N_4O_3$) C, H, N; IR (cm^{-1}) 3237 (m), 3062 (w), 3038 (w), 1655 (s), 1599 (m), 1546 (m), 1517 (s), 1462 (w), 1438 (w), 1343 (m), 1321 (m), 1299 (m), 1271 (m), 1149 (w), 1103 (w), 1062 (w), 1044 (w), 1012 (w), 995 (w), 962 (w), 921 (w), 871 (w), 840 (w), 774 (w), 742 (w), 726 (w), 703 (w), 683 (w), 653 (w), 619 (w), 583 (w); ^{1}H NMR (d_6-DMSO) δ 12.32 (s, 1H, NH), 8.66 (d, 1H, ArH), 8.51 (s, 1H, HC=N), 8.40 (d, 2H, ArH), 8.19 (d, 2H,

ArH), 8.02 (d, 1H, ArH), 7.92 (dd, 1H, ArH), 7.47 (dd, 1H, ArH); MS (ESI) *m/z* 271 (M + H$^+$).

Di-2-pyridylketone *p*-Trifluoromethylbenzoyl Hydrazone (HPKTFH). Equimolar amounts of di-2-pyridyl ketone (0.68 g, 3.7 mmol) and *p*-trifluoromethylbenzoic acid hydrazide (0.76 g, 3.7 mmol) were dissolved in ethanol (70 mL) with stirring. A few drops of concentrated HCl were added as catalyst. The reaction solution was refluxed for 5 h and the product was collected by vacuum filtration, washed with cold ethanol, and air-dried. HPKTFH (85%) was collected as white crystals: Anal. (C$_{19}$H$_{13}$N$_4$OF$_3$) C, H, N; IR (cm^{-1}) 2978 (m), 1684 (s), 1576 (m), 1412 (m), 1320 (s), 1252 (m), 1122 (m), 1065 (w), 1002 (m), 863 (m), 804 (m), 684 (m), 578 (w); ^{1}H NMR (*d$_6$*-DMSO) δ 15.23 (s, 1H, NH), 8.93 (d, 1H, ArH), 8.60 (d, 1H, ArH), 8.09 (d, 2H, ArH), 7.98 (m, 3H, ArH), 7.95 (d, 2H, ArH), 7.62 (dd, 1H, ArH), 7.51 (m, 2H, ArH); MS (ESI) *m/z* 371 (M + H$^+$). All additional HPKIH analogs were prepared in a similar manner.

Di-2-pyridylketone *p*-Nitrobenzoyl Hydrazone (HPKNH). HPKNH (76%) was collected as a yellow powder: Anal. (C$_{18}$H$_{13}$N$_5$O$_3$) C, H, N; IR (cm^{-1}) 3074 (m), 2938 (w), 1700 (s), 1588 (w), 1514 (s), 1462 (m), 1424 (m), 1344 (s), 1320 (m), 1258 (m), 1110 (w), 992 (w), 844 (w), 708 (m), 662 (w); ^{1}H NMR (*d$_6$*-DMSO) δ 15.24 (s, 1H, NH), 8.93 (d, 1H, ArH), 8.60 (d, 1H, ArH), 8.39 (d, 2H, ArH), 8.13 (d, 2H, ArH), 7.98 (m, 3H, ArH), 7.62 (dd, 1H, ArH), 7.51 (m, 2H, ArH); MS (ESI) *m/z* 348 (M + H$^+$).

General Synthesis of the Fe^{II} Complexes. The appropriate ligand (1.1 mmol) was dissolved in 20 mL of acetonitrile and the nonvolatile base, 1,8-diazabicyclo[5.4.0]undec-7-ene (0.17 g, 1.1 mmol) was added while purging with nitrogen. In the case of HMP3BBH and HMPTH, chloroform (20 mL) was used in place of acetonitrile to help dissolve the ligand. Fe(ClO$_4$)$_2$·6H$_2$O (0.2 g, 0.55 mmol) was dissolved in 6 mL of nitrogen-purged acetonitrile and was added with stirring to the ligand solution. The mixture was then gently refluxed under nitrogen for 30 min. In the case of HMP3BBH and HMPTH, most of the chloroform was removed under a nitrogen stream before the reaction was cooled. After cooling, the dark green product was collected by filtration and washed with acetonitrile.

Fe^{II}(MPIH)$_2$. Yield 89%. Anal. (C$_{24}$H$_{20}$FeN$_{10}$O$_2$) C, H, N; IR (cm^{-1}) 3042 (w), 2904 (w), 1597 (m), 1571 (m), 1470 (w), 1427 (s), 1374 (s), 1326 (s), 1309 (s), 1290 (m), 1181 (w), 1151 (s), 1131 (w), 1070 (m), 1040 (m), 1008 (m), 993 (w), 908 (w), 888 (w), 835 (s), 798 (w), 752 (m), 711 (m), 706 (m), 692 (s), 668 (w), 650 (w), 641 (m), 558 (m). Electronic spectrum (CH$_3$CN): λ$_{max}$ (nm; ε L mol^{-1} cm^{-1}) 251 (26900), 269 (24700), 365 (28000), 685 (5100); ^{1}H NMR (*d$_6$*-DMSO) δ 11.64 (s, 1H), 10.91 (s, 1H), 9.11 (s, 3H), 8.6 (overlapping singlets, 4H). The methyl ^{1}H NMR signal was obscured by the solvent DMSO in this and all other complexes. MS (ESI) *m/z* 537 (Fe(MPIH)$_2$ + H$^+$).

Fe^{II}(MPBH)$_2$. Yield 91%. Anal. (C$_{26}$H$_{22}$FeN$_8$O$_2$) C, H, N; IR (cm^{-1}) 3053 (w), 1599 (w), 1574 (m), 1475 (m), 1451 (m), 1417 (m), 1365 (s), 1326 (s), 1291 (m), 1184 (m), 1158 (m), 1139 (m), 1064 (m), 1040 (m), 1006 (m), 962 (w), 943 (w), 902 (m), 831 (m), 796 (m), 762 (w), 708 (s), 690 (s), 643 (m), 609 (w), 568 (w). Electronic spectrum (CH$_3$CN): λ$_{max}$ (nm; ε L mol^{-1} cm^{-1}) 264 (29000), 311 (19100), 380 (27000), 682 (5900); ^{1}H NMR (*d$_6$*-DMSO) δ 10.07 (s, 1H), 9.95 (s, 1H), 8.23 (s, 1H), 7.68 (s, 1H), 7.59 (m, 1H), 6.24 (s, 1H); MS (ESI) *m/z* 534 (Fe(MPBH)$_2$ + H$^+$).

[Fe^{II}(MP3BBH)$_2$]·0.3CHCl$_3$. Yield 48%. Anal. (C$_{26.3}$H$_{20.3}$-Br$_2$ClFeN$_8$O$_2$) C, H, N; IR (cm^{-1}) 3072 (w), 1648 (w), 1574 (m), 1479 (w), 1465 (w), 1438 (m), 1396 (m), 1366 (s), 1325 (m), 1295 (m), 1261 (m), 1179 (w), 1166 (w), 1146 (m), 1064 (m), 1037 (m), 1012 (w), 910 (m), 891 (w), 833 (w), 821 (m), 801 (m), 735 (s), 711 (w), 675 (w), 641 (m), 568 (w). Electronic spectrum (CH$_3$CN): λ$_{max}$ (nm) (ε L mol^{-1} cm^{-1}) 262 (30500), 319 (15900), 369 (30000), 682 (5400); ^{1}H NMR (*d$_6$*-DMSO) δ 11.0 (s, 1H), 10.51 (s, 1H), 8.39 (m, 2H), 7.91 (m, 3H), 7.47 (s, 2H); MS (ESI) *m/z* 690, 692, 694 (Fe(MP3BBH)$_2$ + H$^+$).

Fe^{II}(MP4BBH)$_2$. Yield 96%. Anal. (C$_{26}$H$_{20}$Br$_2$FeN$_8$O$_2$) C, H, N; IR (cm^{-1}) 3054 (w), 1590 (w), 1576 (m), 1487 (w), 1470 (w), 1440 (s), 1374 (s), 1329 (s), 1299 (m), 1289 (m), 1185 (w), 1167

(m), 1143 (s), 1066 (m), 1043 (m), 1008 (s), 903 (m), 844 (m), 824 (m), 799 (m), 749 (s), 711 (m), 688 (w), 645 (m), 617 (w), 569 (w). Electronic spectrum (CH$_3$CN): λ$_{max}$ (nm) (ε L mol^{-1} cm^{-1}) 270 (120000), 372 (112500), 682 (16500). ^{1}H NMR (*d$_6$*-DMSO) δ 10.57, 10.20, 8.20, 7.97; all broad singlets; MS (ESI) *m/z* 690, 692, 694 (Fe(MP4BBH)$_2$ + H$^+$).

[Fe^{II}(MPAH)$_2$]·0.75H$_2$O. Yield 99%. Anal. (C$_{26}$H$_{25.5}$FeN$_{10}$O$_{2.75}$) C, H, N; IR (cm^{-1}) 3451 (w), 3337 (m), 3227 (m), 1642 (m), 1600 (s), 1446 (m), 1405 (m), 1369 (s), 1322 (w), 1167 (s), 1144 (m), 1070 (m), 1040 (m), 1008 (m), 902 (w), 826 (m), 793 (w), 759 (m), 708 (m), 636 (m). Electronic spectrum (CH$_3$CN): λ$_{max}$ (nm) (ε L mol^{-1} cm^{-1}) 264 (525000), 320 (1415000), 411 (76700), 685 (8700). ^{1}H NMR (*d$_6$*-DMSO) δ 10.57 (s, 1H), 9.25 (s, 1H), 8.66 (d, 2H), 7.70 (d, 2H), 6.63 (d, 2H), 5.84 (s, 2H); MS (ESI) *m/z* 565 (Fe(MPAH)$_2$ + H$^+$).

Fe^{II}(MPTFH)$_2$. Yield 91%. Anal. (C$_{28}$H$_{20}$F$_6$FeN$_8$O$_2$) C, H, N; IR (cm^{-1}) 3057 (w), 1619 (w), 1575 (w), 1514 (w), 1473 (m), 1442 (m), 1378 (m), 1324 (s), 1295 (s), 1162 (w), 1121 (s), 1096 (w), 1060 (m), 1041 (m), 1010 (m), 903 (w), 855 (m), 827 (wm), 780 (w), 767 (m), 704 (m), 645 (w), 613 (w), 588 (w). Electronic spectrum (CH$_3$CN): λ$_{max}$ (nm) (ε L mol^{-1} cm^{-1}) 257 (31600), 367 (30500), 414 (16400), 685 (5500). ^{1}H NMR (*d$_6$*-DMSO) δ 10.92 (s, 1H), 10.45 (s, 1H), 8.56 (s, 3H), 8.18 (s, 4H), 7.48 (s, 3H); MS (ESI) *m/z* 671 (Fe(MPTFH)$_2$ + H$^+$).

[Fe^{II}(MPNH)$_2$]·0.5H$_2$O. Yield 87%. Anal. (C$_{26}$H$_{21}$FeN$_{10}$O$_{6.5}$) C, H, N; IR (cm^{-1}) 3070 (w), 1601 (w), 1519 (s), 1477 (w), 1449 (m), 1397 (w), 1368 (m), 1338 (s), 1310 (s), 1165 (m), 1144 (m), 1104 (m), 1064 (m), 1034 (m), 1000 (w), 907 (w), 872 (m), 849 (s), 758 (w), 717 (s), 698 (m), 626 (w), 558 (w). Electronic spectrum (CH$_3$CN): λ$_{max}$ (nm) (ε L mol^{-1} cm^{-1}) 268 (20600), 381 (22700), 692 (2300). ^{1}H NMR (*d$_6$*-DMSO) δ 11.32 (s, 1H), 10.76 (s, 1H), 8.75 (s, 5H), 7.98 (s, 3H); MS (ESI) *m/z* 625 (Fe(MPNH)$_2$ + H$^+$).

[Fe^{II}(MPTH)$_2$]·0.5CHCl$_3$. Yield 93%. Anal. (C$_{22.5}$H$_{18.5}$Cl$_{1.5}$-FeN$_8$O$_2$S$_2$) C, H, N; IR (cm^{-1}) 3069 (w), 3055 (m), 1578 (m), 1525 (m), 1467 (w), 1421 (s), 1375 (m), 1321 (s), 1298 (s), 1224 (w), 1185 (w), 1117 (m), 1092 (w), 1066 (m), 1028 (m), 1010 (w), 969 (w), 885 (w), 849 (m), 838 (m), 791 (w), 765 (w), 739 (s), 708 (s), 642 (m), 623 (m), 610 (w), 573 (w). Electronic spectrum (CH$_3$CN): λ$_{max}$ (nm) (ε L mol^{-1} cm^{-1}) 266 (20000), 308 (19700), 380 (46000), 676 (1400). ^{1}H NMR (*d$_6$*-DMSO) δ 11.43 (s, 1H), 9.62 (s, 1H), 8.90 (s, 2H), 8.48 (s, CHCl$_3$), 8.26 (s, 1H), 8.18 (s, 1H), 7.44 (m, 1H); MS (ESI) *m/z* 547 (Fe(MPTH)$_2$ + H$^+$).

Biological Studies. Cell Culture. The human SK-N-MC neuroepithelioma and MRC-5 fibroblast cell lines were obtained from the American type Culture Collection (ATCC; Rockville, MD). The cells were grown as described.[21,39,59,60]

Preparation of ^{59}Fe-Transferrin. Human transferrin (Tf; Sigma) was labeled with ^{59}Fe (Dupont NEN, MA) to produce ^{59}Fe$_2$-Tf (^{59}Fe-Tf), as previously described.[59,60] Briefly, apotransferrin was saturated with ^{59}Fe using the ferric nitrilotriacetate complex in a molar ratio of 1:10 Fe/nitrilotriacetate. The saturation of Tf with Fe was monitored by UV–vis spectrophotometry using the absorbance at 280 nm (protein) compared with that at 465 nm (Fe-binding site).

The Effect of Chelators on Cellular Iron Metabolism. Briefly, SK-N-MC cells were used to study the ability of the chelators to induce ^{59}Fe mobilization from prelabeled cells and prevent ^{59}Fe uptake from ^{59}Fe-Tf using standard procedures.[17,21,22,33,35,39,48]

^{59}Fe Efflux from SK-N-MC Cells. Iron efflux experiments examining the ability of various chelators to mobilize ^{59}Fe from SK-N-MC cells were performed using established techniques.[21,61] Briefly, following prelabeling of cells with ^{59}Fe-Tf (0.75 µM) for 3 h at 37 °C, the cell cultures were washed four times with ice-cold PBS and then subsequently incubated with each chelator (50 µM) for 3 h at 37 °C. The overlying media containing released ^{59}Fe was then separated from the cells using a pasteur pipet. Radioactivity was measured in both the cell pellet and supernatant using a γ-scintillation counter (Wallac Wizard 3, Turku, Finland). In these studies, the novel ligands were compared to the previously characterized chelators, DFO, H$_2$NIH, and H$_2$PIH HDp44mT, and the HPCIH and HPKIH analogs.[17,21,22,33,36]

Effect of Chelators at Preventing ^{59}Fe Uptake from Tf. The ability of the chelator to prevent cellular ^{59}Fe uptake from the serum Fe transport protein ^{59}Fe-Tf was examined using established techniques.[17,33] Briefly, cells were incubated with ^{59}Fe-Tf (0.75 μM) for 3 h at 37 °C in the presence of each of the chelators (50 μM). The cells were then washed four times with ice-cold PBS and internalized ^{59}Fe was determined by standard techniques by incubating the cell monolayer for 30 min at 4 °C with the general protease, Pronase (1 mg/mL; Sigma).[59,60] The cells were removed from the monolayer using a plastic spatula and centrifuged for 1 min at 14000 rpm. The supernatant represents membrane-bound, Pronase-sensitive ^{59}Fe that was released by the protease, while the Pronase-insensitive fraction represents internalized ^{59}Fe. The novel ligands were compared to the previously characterized chelators, DFO, H$_2$NIH, and HDp44mT and the HPCIH and HPKIH series analogs.[17,21,22,33,39]

Effect of the Chelators on Cellular Proliferation. This was examined using the MTT (3-(4,5-dimethylthiazol-2-yl)-2,5-diphenyl tetrazolium) assay as described.[21,39] MTT color formation was directly proportional to the number of viable cells measured by Trypan blue staining.[21]

Ascorbate Oxidation Assay. An established protocol was used to measure ascorbate oxidation.[23,24,48,62] Briefly, ascorbic acid (100 μM) was prepared immediately prior to an experiment and incubated in the presence of Fe^{III} (10 μM; added as FeCl$_3$), a 50-fold molar excess of citrate (500 μM), and the chelator (1–60 μM) at pH 7.4. Absorbance at 265 nm was measured after 10 and 40 min at room temperature, and the decrease of intensity between these time points was calculated.[48,62]

Benzoate Hydroxylation. This assay employs benzoate as a hydroxyl radical scavenger to generate fluorescent salicylate as a product (308 nm excitation and 410 nm emission) using a well-established protocol.[23,24,48,62] Briefly, benzoic acid (1 mM) was incubated for 1 h at room temperature in 10 mM disodium hydrogen phosphate (pH 7.4) with 5 mM hydrogen peroxide, the Fe chelator (3−180 μM), and ferrous sulfate (30 μM) at pH 7.4. All solutions were prepared immediately prior to use and the Fe^{II} added to water that had been extensively purged with nitrogen. The addition of Fe was used to start the reaction, and the solution was kept in the dark prior to measuring the fluorescence using a Perkin-Elmer L550B spectrofluorometer. In these experiments, salicylate was used as a standard and to determine quenching by the chelators.[48,62]

Statistical Analysis. Experimental data were compared using Student's t-test. Results were expressed as mean or mean ± SD (number of experiments) and were considered to be statistically significant when $p < 0.05$.

Supporting Information Available: Elemental analysis data. This material is available free of charge via the Internet at http://pubs.acs.org.

References

(1) Bergeron, R. J.; Bharti, N.; Wiegand, J.; McManis, J. S.; Yao, H.; Prokai, L. Polyamine-vectored iron chelators: The role of charge. *J. Med. Chem.* **2005**, *48*, 4120–4137.

(2) Bergeron, R. J.; Wiegand, J.; Bharti, N.; Singh, S.; Rocca, J. R. Impact of the 3,6,9-trioxadecyloxy group on desazadesferrithiocin analogue iron clearance and organ distribution. *J. Med. Chem.* **2007**, *50*, 3302–3313.

(3) Bergeron, R. J.; Wiegand, J.; McManis, J. S.; Bharti, N. The design, synthesis, and evaluation of organ-specific iron chelators. *J. Med. Chem.* **2006**, *49*, 7032–7043.

(4) Bernhardt, P. V. Coordination chemistry and biology of chelators for the treatment of iron overload disorders. *Dalton Trans.* **2007**, 3214–3220.

(5) Kalinowski, D. S.; Richardson, D. R. The evolution of iron chelators for the treatment of iron overload disease and cancer. *Pharmacol. Rev.* **2005**, *57*, 547–583.

(6) Aouad, F.; Florence, A.; Zhang, Y.; Collins, F.; Henry, C.; Ward, R. J.; Crichton, R. R. Evaluation of new iron chelators and their therapeutic potential. *Inorg. Chim. Acta* **2002**, *339*, 470–480.

(7) Hershko, C.; Abrahamov, A.; Konijn, A. M.; Breuer, W.; Cabantchick, I. Z.; Pootrakul, P.; Link, G. Objectives and methods of iron chelation therapy. *Bioinorg. Chem. Appl.* **2003**, *1*, 151–168.

(8) Olivieri, N. F.; Brittenham, G. M. Iron-chelating therapy and the treatment of thalassemia. *Blood* **1997**, *89*, 739–761.

(9) Wong, C.; Richardson, D. R. Beta-thalassaemia: Emergence of new and improved iron chelators for treatment. *Int. J. Biochem. Cell Biol.* **2003**, *35*, 1144–1149.

(10) Kontoghiorghes, G. J.; Pattichis, K.; Neocleous, K.; Kolnagou, A. The design and development of deferiprone (L1) and other iron chelators for clinical use: Targeting methods and application prospects. *Curr. Med. Chem.* **2004**, *11*, 2161–2183.

(11) Richardson, D. R. The controversial role of deferiprone in the treatment of thalassemia. *J. Lab. Clin. Med.* **2001**, *137*, 324–329.

(12) Olivieri, N. F.; Brittenham, G. M.; McLaren, C. E.; Templeton, D. M.; Cameron, R. G.; McClelland, R. A.; Burt, A. D.; Fleming, K. A. Long-term safety and effectiveness of iron-chelation therapy with deferiprone for thalassemia major. *N. Engl. J. Med.* **1998**, *339*, 417–423.

(13) Maggio, A.; D'Amico, G.; Morabito, A.; Capra, M.; Ciaccio, C.; Cianciulli, P.; Di Gregorio, F.; Garozzo, G.; Malizia, R.; Magnano, C.; et al. Deferiprone versus deferoxamine in patients with thalassemia major: A randomized clinical trial. *Blood Cells Mol. Dis.* **2002**, *28*, 196–208.

(14) Wanless, I. R.; Sweeney, G.; Dhillon, A. P.; Guido, M.; Piga, A.; Galanello, R.; Gamberini, M. R.; Schwartz, E.; Cohen, A. R. Lack of progressive hepatic fibrosis during long-term therapy with deferiprone in subjects with transfusion-dependent beta-thalassemia. *Blood* **2002**, *100*, 1566–1569.

(15) Nick, H. Iron chelation, quo vadis? *Curr. Opin. Chem Biol.* **2007**, in press.

(16) Kontoghiorghes, G. J. Deferasirox: Uncertain future following renal failure fatalities, agranulocytosis and other toxicities. *Expert Opin. Drug Saf.* **2007**, *6*, 235–239.

(17) Becker, E.; Richardson, D. R. Development of novel aroylhydrazone ligands for iron chelation therapy: 2-pyridylcarboxaldehyde isonicotinoyl hydrazone analogs. *J. Lab. Clin. Med.* **1999**, *134*, 510–521.

(18) Bernhardt, P. V.; Chin, P.; Sharpe, P. C.; Richardson, D. R. Hydrazone chelators for the treatment of iron overload disorders: iron coordination chemistry and biological activity. *Dalton Trans.* **2007**, 3232–3244.

(19) Richardson, D. R.; Mouralian, C.; Ponka, P.; Becker, E. Development of potential iron chelators for the treatment of Friedreich's ataxia: ligands that mobilize mitochondrial iron. *Biochim. Biophys. Acta* **2001**, *1536*, 133–140.

(20) Wong, C. S.; Kwok, J. C.; Richardson, D. R. PCTH: A novel orally active chelator of the aroylhydrazone class that induces iron excretion from mice. *Biochim. Biophys. Acta* **2004**, *1739*, 70–80.

(21) Richardson, D. R.; Tran, E. H.; Ponka, P. The potential of iron chelators of the pyridoxal isonicotinoyl hydrazone class as effective antiproliferative agents. *Blood* **1995**, *86*, 4295–4306.

(22) Becker, E. M.; Lovejoy, D. B.; Greer, J. M.; Watts, R.; Richardson, D. R. Identification of the di-pyridyl ketone isonicotinoyl hydrazone (PKIH) analogues as potent iron chelators and anti-tumour agents. *Br. J. Pharmacol.* **2003**, *138*, 819–830.

(23) Bernhardt, P. V.; Caldwell, L. M.; Chaston, T. B.; Chin, P.; Richardson, D. R. Cytotoxic iron chelators: characterization of the structure, solution chemistry and redox activity of ligands and iron complexes of the di-2-pyridyl ketone isonicotinoyl hydrazone (HPKIH) analogues. *J. Biol. Inorg. Chem.* **2003**, *8*, 866–880.

(24) Chaston, T. B.; Watts, R. N.; Yuan, J.; Richardson, D. R. Potent antitumor activity of novel iron chelators derived from di-2-pyridylketone isonicotinoyl hydrazone involves fenton-derived free radical generation. *Clin. Cancer Res.* **2004**, *10*, 7365–7374.

(25) Richardson, D. R.; Becker, E.; Bernhardt, P. V. The biologically active iron chelators 2- pyridylcarboxaldehyde isonicotinoyl hydrazone, 2-pyridylcarboxaldehyde benzoyl hydrazone and 2-furfural isonicotinoyl hydrazone. *Acta Crystallogr., Sect. C: Cryst. Struct. Commun.* **1999**, *C55*, 2102–2105.

(26) Armstrong, C. M.; Bernhardt, P. V.; Chin, P.; Richardson, D. Structural variations and formation constants of first-row transition metal complexes of biologically active aroylhydrazones. *Eur. J. Inorg. Chem.* **2003**, 1145–1156.

(27) Bernhardt, P. V.; Wilson, G. J.; Sharpe, P. C.; Kalinowski, D. S.; Richardson, D. R. Tuning the anti-proliferative activity of biologically active iron chelators: Characterisation of the coordination chemistry and biological efficacy of 2-acetylpyridine and 2-benzoylpyridine hydrazone ligands. *J. Biol. Inorg. Chem.* **2008**, *13*, 107–119.

(28) Bernhardt, P. V.; Chin, P.; Sharpe, P. C.; Wang, J.-Y. C.; Richardson, D. R. Novel diaroylhydrazine ligands as iron chelators: coordination chemistry and biological activity. *J. Biol. Inorg. Chem.* **2005**, *10*, 761–777.

(29) Edward, J. T.; Chubb, F. L.; Sangster, J. Iron chelators of the pyridoxal isonicotinoyl hydrazone class. Relationship of the lipophilicity of the apochelator to its ability to mobilize iron from reticulocytes in vitro: reappraisal of reported partition coefficients. *Can. J. Physiol. Pharmacol.* **1997**, *75*, 1362–1368.

(30) Kalinowski, D. S.; Richardson, D. R. Future of toxicology-iron chelators and differing modes of action and toxicity: The changing face of iron chelation therapy. *Chem. Res. Toxicol.* **2007**, *20*, 715–720.

(31) Richardson, D. R.; Sharpe, P. C.; Lovejoy, D. B.; Senaratne, D.; Kalinowski, D. S.; Islam, M.; Bernhardt, P. V. Dipyridyl thiosemicarbazone chelators with potent and selective antitumor activity form iron complexes with redox activity. *J. Med. Chem.* **2006**, *49*, 6510–6521.

(32) Kalinowski, D. S.; Yu, Y.; Sharpe, P. C.; Islam, M.; Liao, Y. T.; Lovejoy, D. B.; Kumar, N.; Bernhardt, P. V.; Richardson, D. R. Design, synthesis, and characterization of novel iron chelators: Structure−activity relationships of the 2-benzoylpyridine thiosemicarbazone series and their 3-nitrobenzoyl analogues as potent antitumor agents. *J. Med. Chem.* **2007**, *50*, 3716–3729.

(33) Yuan, J.; Lovejoy, D. B.; Richardson, D. R. Novel di-2-pyridyl-derived iron chelators with marked and selective antitumor activity: In vitro and in vivo assessment. *Blood* **2004**, *104*, 1450–1458.

(34) Whitnall, M.; Howard, J.; Ponka, P.; Richardson, D. R. A class of iron chelators with a wide spectrum of potent anti-tumor activity that overcome resistance to chemotherapeutics. *Proc. Natl. Acad. Sci. U.S.A.* **2006**, *103*, 14901–14906.

(35) Darnell, G.; Richardson, D. R. The potential of iron chelators of the pyridoxal isonicotinoyl hydrazone class as effective antiproliferative agents III: The effect of the ligands on molecular targets involved in proliferation. *Blood* **1999**, *94*, 781–792.

(36) Richardson, D. R.; Ponka, P. The iron metabolism of the human neuroblastoma cell: lack of relationship between the efficacy of iron chelation and the inhibition of DNA synthesis. *J. Lab. Clin. Med.* **1994**, *124*, 660–671.

(37) Ponka, P.; Borova, J.; Neuwirt, J.; Fuchs, O. Mobilization of iron from reticulocytes. Identification of pyridoxal isonicotinoyl hydrazone as a new iron chelating agent. *FEBS Lett.* **1979**, *97*, 317–321.

(38) Ponka, P.; Borova, J.; Neuwirt, J.; Fuchs, O.; Necas, E. A study of intracellular iron metabolism using pyridoxal isonicotinoyl hydrazone and other synthetic chelating agents. *Biochim. Biophys. Acta* **1979**, *586*, 278–297.

(39) Richardson, D. R.; Milnes, K. The potential of iron chelators of the pyridoxal isonicotinoyl hydrazone class as effective antiproliferative agents II: The mechanism of action of ligands derived from salicylaldehyde benzoyl hydrazone and 2-hydroxy-1-naphthylaldehyde benzoyl hydrazone. *Blood* **1997**, *89*, 3025–3038.

(40) Yu, Y.; Wong, J.; Lovejoy, D. B.; Kalinowski, D. S.; Richardson, D. R. Chelators at the cancer coalface: Desferrioxamine to triapine and beyond. *Clin. Cancer Res.* **2006**, *12*, 6876–6883.

(41) Lovejoy, D. B.; Richardson, D. R. Novel "hybrid" iron chelators derived from aroylhydrazones and thiosemicarbazones demonstrate selective antiproliferative activity against tumor cells. *Blood* **2002**, *100*, 666–676.

(42) Feun, L.; Modiano, M.; Lee, K.; Mao, J.; Marini, A.; Savaraj, N.; Plezia, P.; Almassian, B.; Colacino, E.; Fischer, J.; et al. Phase I and pharmacokinetic study of 3-aminopyridine-2-carboxaldehyde thiosemicarbazone (3-AP) using a single intravenous dose schedule. *Cancer Chemother. Pharmacol.* **2002**, *50*, 223–229.

(43) Chaston, T. B.; Lovejoy, D. B.; Watts, R. N.; Richardson, D. R. Examination of the antiproliferative activity of iron chelators: Multiple cellular targets and the different mechanism of action of triapine compared with desferrioxamine and the potent pyridoxal isonicotinoyl hydrazone analogue 311. *Clin. Cancer Res.* **2003**, *9*, 402–414.

(44) Richardson, D. R.; Bernhardt, P. Crystal and molecular structure of 2-hydroxy-1-naphthylaldehyde isonicotinoyl hydrazone (NIH) and its iron(III) complex: An iron chelator with anti-proliferative activity. *J. Biol. Inorg. Chem.* **1999**, *4*, 266–273.

(45) Bernhardt, P. V.; Mattsson, J.; Richardson, D. R. Complexes of cytotoxic chelators from the dipyridyl ketone isonicotinoyl hydrazone (HPKIH) analogues. *Inorg. Chem.* **2006**, *45*, 752–760.

(46) Johnson, D. K.; Pippard, M. J.; Murphy, T. B.; Rose, N. J. An in vivo evaluation of iron-chelating drugs derived from pyridoxal and its analogs. *J. Pharmacol. Exp. Ther.* **1982**, *221*, 399–403.

(47) Richardson, D. R. Cytotoxic analogs of the iron(III) chelator pyridoxal isonicotinoyl hydrazone: effects of complexation with copper(II), gallium(III), and iron (III) on their antiproliferative activities. *Antimicrob. Agents Chemother.* **1997**, *41*, 2061–2063.

(48) Chaston, T. B.; Richardson, D. R. Interactions of the pyridine-2-carboxaldehyde isonicotinoyl hydrazone class of chelators with iron and DNA: Implications for toxicity in the treatment of iron overload disease. *J. Biol. Inorg. Chem.* **2003**, *8*, 427–438.

(49) Bernhardt, P. V.; Chin, P.; Richardson, D. R. Unprecedented oxidation of a biologically active aroylhydrazone chelator catalysed by iron(III): Serendipitous identification of diacylhydrazine ligands with high iron chelation efficacy. *J. Biol. Inorg. Chem.* **2001**, *6*, 801–809.

(50) Chaston, T. B.; Richardson, D. R. Iron chelators for the treatment of iron overload disease: Relationship between structure, redox activity, and toxicity. *Am. J. Hematol.* **2003**, *73*, 200–210.

(51) St Pierre, T. G.; Richardson, D. R.; Baker, E.; Webb, J. A low-spin iron complex in human melanoma and rat hepatoma cells and a high-spin iron(II) complex in rat hepatoma cells. *Biochim. Biophys. Acta* **1992**, *1135*, 154–158.

(52) Klausner, R. D.; Van Renswoude, J.; Ashwell, G.; Kempf, C.; Schechter, A. N.; Dean, A.; Bridges, K. R. Receptor-mediated endocytosis of transferrin in K562 cells. *J. Biol. Chem.* **1983**, *258*, 4715–4724.

(53) Fleming, M. D.; Trenor, C. C., III; Su, M. A.; Foernzler, D.; Beier, D. R.; Dietrich, W. F.; Andrews, N. C. Microcytic anaemia mice have a mutation in Nramp2, a candidate iron transporter gene. *Nat. Genet.* **1997**, *16*, 383–386.

(54) Edward, J. T.; Gauthier, M.; Chubb, F. L.; Ponka, P. Synthesis of new acylhydrazones as iron-chelating compounds. *J. Chem. Eng. Data* **1988**, *33*, 538–540.

(55) Bacchi, A.; Carcelli, M.; Costa, M.; Pelagatti, P.; Pelizzi, C.; Pelizzi, G. Versatile ligand behaviour of phenyl 2-pyridyl ketone benzoylhydrazone in palladium (II) complexes. *J. Chem. Soc., Dalton Trans.* **1996**, *22*, 492–501.

(56) Farrugia, L. J. WinGX suite for small-molecule single crystal crystallography. *J. Appl. Crystallogr.* **1999**, *32*, 837–838.

(57) Sheldrick, G. M. *SHELX97: programs for crystal structure analysis*, release 97-2; University of Gottingen: Germany, 1997.

(58) Farrugia, L. J. ORTEP-3 for windows -a version of ORTEP-III with a graphical user interface (GUI). *J. Appl. Crystallogr.* **1997**, *30*, 565.

(59) Richardson, D. R.; Baker, E. The uptake of iron and transferrin by the human malignant melanoma cell. *Biochim. Biophys. Acta* **1990**, *1053*, 1–12.

(60) Richardson, D. R.; Baker, E. Intermediate steps in cellular iron uptake from transferrin. Detection of a cytoplasmic pool of iron, free of transferrin. *J. Biol. Chem.* **1992**, *267*, 21384–21389.

(61) Baker, E.; Richardson, D.; Gross, S.; Ponka, P. Evaluation of the iron chelation potential of hydrazones of pyridoxal, salicylaldehyde and 2-hydroxy-1-naphthylaldehyde using the hepatocyte in culture. *Hepatology* **1992**, *15*, 492–501.

(62) Dean, R. T.; Nicholson, P. The action of nine chelators on iron-dependent radical damage. *Free Radical Res.* **1994**, *20*, 83–101.